Article type: Research Article

Title: *Serendipita indica* drives sulfur-related microbiota in enhancing growth of hyperaccumulator *Sedum alfredii* and facilitating soil cadmium remediation

Running title: *Serendipita indica* recruits sulfur-related microbiota for phytoremediation

Authors' names: Yabei Qiao[1,2], Zhi Lin[1,2], Luxi Li[3], Wei Jiang[4], Jun Ge[1,2], Jiuzhou Chen[1,2], Lingli Lu[1,2], Shengke Tian[1,2]*

Author affiliations:

[1] MOE Key Laboratory of Environment Remediation and Ecological Health, College of Environmental & Resource Science, Zhejiang University, Hangzhou 310058, P.R. China.

[2] Zhejiang Provincial Key Laboratory of Subtropic Soil and Plant Nutrition, Zhejiang University, Hangzhou 310058, P.R. China.

[3] Advanced Photon Source, Argonne National Laboratory, Lemont, Illinois 60439, USA.

[4] Xianghu Laboratory, Biotechnology Institute, Hangzhou 311231, P.R. China.

*** Corresponding author:**

Shengke Tian, E-mail: tiansk@zju.edu.cn

Address: 866 Yuhangtang Rd, Hangzhou 310058, P.R. China

Tel: 86-571-88982515

Mobile: 86-15700123781

Orcid:

Shengke Tian: https://orcid.org/0000-0001-8242-3581

Yabei Qiao: https://orcid.org/0000-0002-1529-0392

Table of Contents Graphic

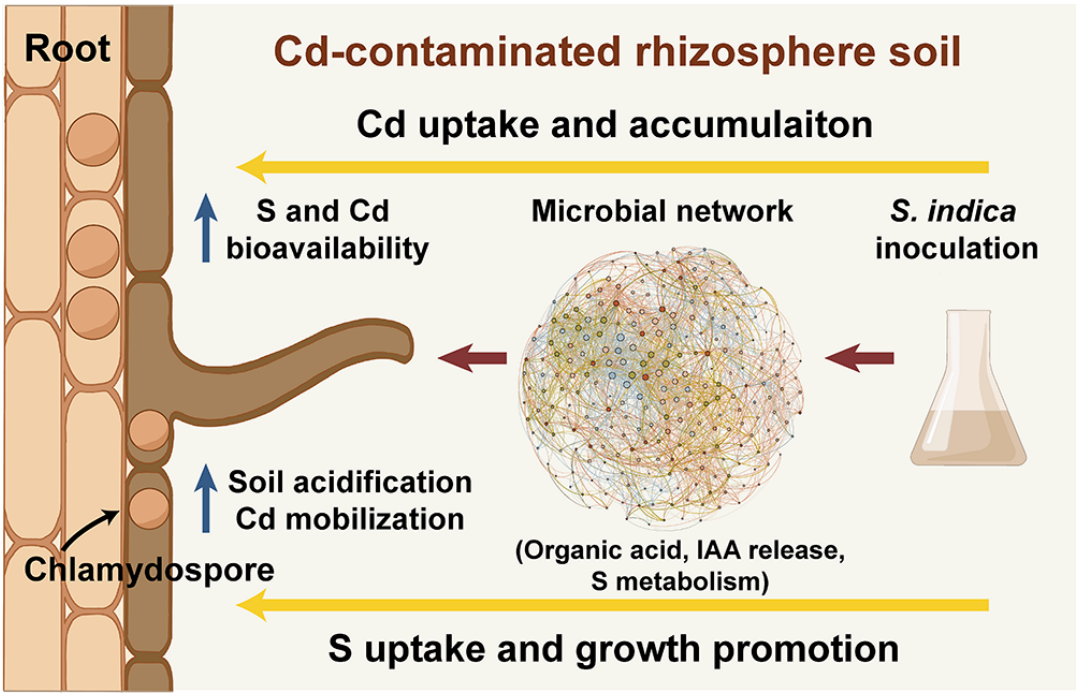

Abstract

Endophytic fungus *Serendipita indica* can bolster plant growth and confer protection against various biotic and abiotic stresses. However, *S. indica*-reshaped rhizosphere microecology interactions and root-soil interface processes *in situ* at the submicron scale remain poorly understood. We combined amplicon sequencing and high-resolution nano x-ray fluorescence (nano-XRF) imaging of the root-soil interface to reveal cadmium (Cd) rhizosphere processes. *S. indica* can successfully colonize the roots of *Sedum alfredii* Hance, which induces a remarkable increase in shoot biomass by 211.32% and Cd accumulation by 235.72%. Nano-XRF images showed that *S. indica* colonization altered Cd distribution in the rhizosphere and facilitated the proximity of more Cd and sulfur (S) to enter the roots and transport to the shoot. Furthermore, the rhizosphere-enriched microbiota demonstrated a more stable network structure after *S. indica* inoculation. Keystone species were strongly associated with growth promotion and Cd absorption. For example, Comamonadaceae are closely related to the organic acid cycle and S bioavailability, which could facilitate Cd and S accumulation in plants. Meanwhile, Sphingomonadaceae could release auxin and boost plant biomass. In summary, we construct a mutualism system

for beneficial fungi and hyperaccumulation plants, which facilitates high-efficient remediation of Cd-contaminated soils by restructuring the rhizosphere microbiota.

Keywords

Nano-XRF, Root-soil interface, Endophytic fungus, *in situ* visualization, Phytoremediation

Synopsis

Beneficial fungi-hyperaccumulator plants mutualism system can significantly augment phytoremediation efficiency of cadmium by increasing soil sulfur migration and reshaping the rhizosphere microbiota, which contributes to the safe production of farmland.

1. Introduction

Soil cadmium (Cd) contamination has evolved into a significant and urgent global problem [1]. Cd, known for its high toxicity and environmental mobility, can accumulate in diverse crops, thereby posing a substantial threat to both human health and the environment [2, 3]. Long-term consumption of Cd-contaminated rice has led to the itai-itai disease, which is characterized by weakened and brittle bones [4, 5]. Consequently, effective countermeasures are required for remediating Cd-contaminated soil. Phytoremediation, employing hyperaccumulator plants, offers an environmentally friendly and cost-effective approach compared to physical, chemical, and other biological methods [6-9]. Hyperaccumulator plants can transfer or immobilize heavy metals in the soil, thereby mitigating their adverse impacts on ecosystems [10].

As a native Cd hyperaccumulator in China, *Sedum alfredii* Hance holds significant potential for usage in the remediation of polluted sites [11] and exhibits great Cd extraction efficiency [12]. *S. alfredii* achieves exceptionally high Cd concentrations in its young leaves and stems due to its efficient mechanisms of root uptake, xylem loading, and phloem remobilization of Cd [13, 14]. However, phytoremediation effectiveness is constrained by the slow growth and low biomass [15]. Thus, the optimization of phytoremediation technology hinges on the promotion plant of growth. One of the most promising and sustainable approaches is the inoculation of plant-growth-promoting microorganisms (PGPM) into the rhizosphere [16]. This approach is known for its cost-effectiveness, environmental friendliness, and low risk [17], which not only significantly bolsters plant resistance against various environmental stressors (e.g., drought, salinity, and heavy metals), but also improves overall plant growth and yield [18-20]. Previous studies have pointed out its significant enhancements in germination rates, seedling survival, and plant biomass [21-23]. PGPMs also regulate heavy metal bioavailability through the production of siderophores, organic acids, and biosurfactants, as well as stimulating the release of root exudates [24]. Additionally, heavy metal-resistant endophytes have been shown to enhance the mobilization of Pb in the rhizosphere, further contributing to phytoremediation efficiency [25]. Moreover,

when endophytes are added to heavy metal-contaminated soil, they can change the structure and composition of microbial community. Previous researches have highlighted the key role of microbiota in *S. alfredii* rhizosphere, with specific focus on the bacterial and archaeal communities, in controlling the bioavailability, uptake, and transformation processes of essential nutrients and metal [26-28]. Since the enhancement of phytoremediation efficiency is associated with microbe species [29, 30], it is necessary to raise the core strains for phytoremediation.

Serendipita indica (formerly known as *Piriformospora indica*), a fungus belonging to the Serendipitaceae family within the order Sebacinales [31], has been extensively studied as a root-colonizing fungus with a wide range of beneficial effects on numerous host plants [32, 33]. This fungal species establishes symbiotic associations with a broad spectrum of over 200 plant species, facilitating plant growth and improving nutrient and water absorption [34]. Furthermore, this mutualistic association protects against pathogens and mitigates the adverse effects of various stressors, including acidity, desiccation, and heavy metal toxicity [35]. Shahabivand, et al. demonstrated that *S. indica* effectively improves the tolerance of sunflower (*Helianthus annuus* L.) to Cd toxicity by immobilizing Cd in the root system [36]. Meanwhile, *S. indica* can alter root-associated microbiome structure to protect plant growth and enhance phytoremediation, such as king grass (*Pennisetum purpureum* × *P. americanum*) and *Artemisia annua* L. [37-39]. *S. indica* also plays a key role in enhancing plant sulfur (S) nutrition. S nutrition is a key element in conferring stress tolerance and promoting heavy metal detoxification [40, 41]. This is important for improving the stress adaptation and detoxification capabilities of hyperaccumulator plants and enhancing the phytoremediation. However, it is still unknown whether *S. indica* can enhance phytoremediation by reshaping the microecology of the rhizosphere microbial community of the hyperaccumulator plants. Hence, it is essential to elucidate the mechanisms governing Cd tolerance, absorption, and rhizosphere microbiota in the symbiotic system of hyperaccumulators and *S. indica*. This aimed was to increase the efficiency of phytoremediation and safeguard agricultural production on contaminated farmlands.

In our research, we harnessed the Cd hyperaccumulator *S. alfredii* as the plant and the endophyte *S. indica* as a fungal inoculant for the remediation of Cd-contaminated soils. We aim: I) to evaluate the phytoremediation potential of the hyperaccumulator *S. alfredii* and the endophyte *S. indica* in a pot system by measuring plant biomass and determining Cd accumulation, etc.; II) to investigate how the rhizosphere microbial community affects element migration and absorption at the root-soil interface under *S. indica* treatment utilizing synchrotron-based X-ray fluorescence (SR-XRF) *in situ* imaging at the submicron scales; III) to explore the correlation between phytoremediation efficiency and rhizosphere microecological characteristic.

2. Materials and methods

2.1. Soil materials

We collected topsoil (0−20 cm) from a disused farmland near Hangzhou, China, where crop growth is impaired due to heavy metal contamination resulting from mining activities. The initial soil properties are as follows: pH 7.4, total carbon content of 18.12 $g \cdot kg^{-1}$, total phosphorus content of 472.63 $mg \cdot kg^{-1}$, total nitrogen content of 10.07 $g \cdot kg^{-1}$, S content of 310.23 $mg \cdot kg^{-1}$, total Cd content of 6.47 $mg \cdot kg^{-1}$, and cation exchange capacity (CEC) of 16.60 cmol (+) $\cdot kg^{-1}$. According to the regulations provided in China's Environmental Quality Evaluation Standards for Farmland of Edible Agricultural Products (HJ/T 332-2006) and the Environmental Quality Standard for Soils of China (GB 15618-1995), the soil was categorized as severely contaminated with Cd.

2.2. Plant growth and *S. indica* co-cultivation

S. alfredii seedlings were sourced from a historical Pb/Zn mining site in Quzhou, Zhejiang Province, China. It was reported as a powerful Cd hyperaccumulator and can offer a useful plant material for phytoremediation of Cd-contaminated soils [11]. To reduce internal metal content, these seedlings were grown for more than three generations in uncontaminated soil. Subsequently, we selected healthy and uniformly sized plant shoots for two-week pre-cultivation in a basic nutrient solution to facilitate root development, as outlined in Lu, et al. [28].

The *S. indica* strain was kindly provided by Prof. Wenying Zhang from Yangtze University, China. To cultivate the *S. indica* mycelium, we utilized a modified liquid *Aspergillus* medium [42] and maintained it at 28 ± 2°C with agitating at 150 rpm in an orbital shaker, and incubated in the absence of light for two weeks [43]. Fresh mycelia were harvested from the liquid medium, weighed, and subsequently diluted to a concentration of 250 $mg \cdot mL^{-1}$ using sterile water. To aid in the grinding process, one steel bead (Ø 2.0 – 4.0 mm) was added per milliliter of the mycelial suspension before undergoing two cycles of grinding, each lasting for 10 seconds at a frequency of 50 Hz, employing a rotor-stator homogenizer (Shanghai Wonbio Biotechnology). The mycelium was washed twice with nine volumes of water, followed by centrifugation at 700 × g for 2 minutes. The final pellets were resuspended in sterile water and adjusted to a concentration of 1 $g \cdot L^{-1}$.

After homogeneous *S. alfredii* seedlings were transplanted into pots (Fig. 1b), *S. indica*-treated microcosms were inoculated with 1.6 mL of a mycelial suspension, containing 100 mg of mycelium per pot, using a pipettor (Fig. 1c) as described [44]. The control pots received an equivalent volume of sterile water as an amendment.

2.3. Pot experiment design

The experiment was conducted in the greenhouse located at Zijingang Campus, Zhejiang University, Zhejiang, China. Controlled environmental conditions included a 16/8-hour light/dark cycle, day/night temperatures of 30/24°C, relative humidity levels of 70%/85%, and a photon flux density of 400 $\mu mol \cdot m^{-2} \cdot s^{-1}$.

The treatments included the following: (i) unplanted soil (unplanted, Un); (ii) *S. alfredii*-planted soil without *S. indica* (control, CK); (iii) *S. alfredii*-planted soil inoculated with *S. indica* (+*Si*); (iv) *S. alfredii*-planted γ-irradiated soil without *S. indica; (v) S. alfredii*-planted γ-irradiated soil inoculated with *S. indica*. The soil samples were subjected to air-drying, passed through a 2 mm sieve, and placed into plastic pots measuring 13.00 cm in diameter and 14.50 cm in height. To distinct between the rhizosphere and bulk soil, we used a polyester mesh root bag with a pore size of 300 mesh, measuring 8 cm in diameter and 18 cm in height. The root bag was filled with 200 g of soil and positioned within each pot. To surround the root bags, an

additional 550 g of soil was integrated as bulk soil (Fig. 1a). Nylon meshes were placed between the compartments to constrain root hair movement while ensuring unobstructed water and solute passage. To uphold soil moisture at around 60% of its water-holding capacity, deionized water was utilized. Each treatment was replicated in six separate pots, and these pots were randomly arranged for the experiment.

2.4. Soil sampling and plant harvesting

Following a 60-day cultivation period, the plants were harvested. We collected rhizosphere soil by shaking the plant roots and placing the soil adhering to the roots into a 20 ml phosphate-buffered saline solution. The rhizosphere compartment was formed from the soil dislodged from the plant roots, and the bulk soil was collected from the outer layer of the soil. Subsequently, the plant and soil samples were transported to the laboratory on dry ice. After transport, the samples were stored at a temperature of -80°C until the extraction of DNA was conducted. More details about elemental analyses are shown in *Supplementary Materials and Methods*.

2.5. Histochemical analysis

To visualize the colonization of roots by *S. indica*, we initially treated fresh root samples by immersing them in a 10% KOH solution for 15 min, followed by acidification using 1 M HCl for another 10 min. Then these samples were examined using a light microscope (Nikon, Tokyo, Japan). Detecting chlamydospores within the roots provided a clear indication of successful colonization (refer to Supplemental Fig. S1).

2.6. Element Mapping by Nano-XRF

We sliced the root-soil interface samples to a thickness of 120 μm for Nano-XRF analysis using a cryotome (CM1950, Leica Biosystems) at -20°C, as described [45]. Nano-XRF imaging was executed (Fig. 1d) at the Advanced Photon Source 2-ID-D hard X-ray microprobe beamlines within a helium atmosphere [46, 47].X-rays with an incident energy of 28 keV were employed to excite elements varying from potassium (K) to Cd. Utilizing a Fresnel zone plate, we focused the X-ray beam onto the sample, achieving a spot size of 1 × 1 μm and 500 × 500 nm. The sample image was then systematically raster-scanned, with each pixel having a dwell time of 10 ms. The

X-ray fluorescence emitted by the sample was collected using an energy-dispersive silicon drift detector. Subsequently, maps depicting the distribution of Cd, K, and S were generated and analyzed using the MAPS software [48]. More procedures are showed in *Supplementary Materials and Methods*.

2.7. DNA extraction and amplicon sequencing

Soil genomic DNA was isolated using the MOBIO DNeasy PowerSoil kit (Qiagen, Valencia, CA, USA). Subsequently, we quantified the DNA samples by spectrophotometry, using a Nanodrop spectrophotometer (Nanodrop Technologies Inc., Wilmington, DE, USA), and then stored at -80°C before the amplification process (Fig. 1d). The amplification of the V3-V4 regions of bacterial 16S rRNA genes was carried out using the primer sets 338F (5′-ACTCCTACGGGAGGCAGCA-3′) and 806R (5′-GGACTACHVGGGTWTCTAAT-3′) [49, 50]. The fungal ITS1 region were amplified using primers ITS1F (5′-CTTGGTCATTTAGAGGAAGTAA-3′) and ITS2-2043R (5′-GCTGCGTTCTTCATCGATGC-3′) [51].

PCR reactions were conducted following the established protocol [52]. We performed high-throughput sequencing of PCR amplicons using 250bp paired-end sequencing on the Illumina HiSeq 2500 platform (Guangdong Magigene Biotechnology Co., Ltd. Guangzhou, China) (Fig. 1d). Microbiome 16S rRNA and ITS gene sequencing were analyzed utilizing the Quantitative Insights into Microbial Ecology 2 (QIIME2) platform [53]. Initially, raw reads underwent demultiplexing using the "q2-demux" plugin. Subsequently, the sequences were subjected to denoising employing the DADA2 algorithm. The "q2-dada2" plugin [54] was utilized to get a table of amplicon sequence variants (ASVs).

ASVs were then annotated by aligning them with the SILVA reference database version 138 for bacteria [55] and the UNITE database version 6.0 for fungi (https://unite.ut.ee/) [56]. ASVs from chloroplasts or mitochondria were excluded from the subsequent analysis.

2.8. Data analysis

To examine the variations in plant and soil parameters among different soil

compartments, SPSS 26.0 (IBM Corp., Armonk, NY, USA) was used for statistical analysis. We used the Shapiro-Wilk test to assess the normality of the residuals and the Levene's test to evaluate the homoscedasticity of the data. We conducted student's t-test or analysis of variance and subsequently performed post hoc comparisons with Tukey's Honestly Significant Difference test. The translocation factor (TF) and the bioaccumulation factor (BF) were calculated to quantify the efficiency of phytoextraction and evaluate the capacity of transporting or accumulating Cd [57, 58]. TF value represents the ratio of contaminant concentration in the plant shoots to that in the roots, while the BF denotes the ratio of contaminant concentration in the plant to that in the soil. We utilized Origin v2019b (OriginLab Corp., Northampton, MA, USA) to visualize the relative abundances of bacterial and fungal communities via 100% stacked columns. For statistical analysis and figure generation, we employed the R program v4.3.0 (http://www.r-project.org/). More statistical analyses are showed in *Supplementary Materials and Methods*.

2.9. Network construction based on the random matrix theory

We conducted microbial co-occurrence network analysis employing Spearman's correlation method to distinguish pairwise associations among ASVs [59]. ASVs with relative abundances below 0.02% were excluded. Afterward, we applied the Benjamini–Hochberg FDR control procedure [60] to adjust *p* values for multiple comparisons. To establish Spearman correlation thresholds, we employed the Random Matrix Theory (RMT) method [61]. Finally, correlations were retained if their adjusted *p*-value was below 0.05, and they achieved a score above the specified threshold. Network properties were computed using the Molecular Ecological Network Analysis pipeline (MENA, http://ieg2.ou.edu/MENA/) [62].

3. Results and Discussion

S. indica plays a significant role in enhancing plant growth and heavy metal accumulation, benefiting phytoremediation strategies [38]. This fungal endophyte is known to improve nutrient uptake [40, 44, 63], modulate hormone levels [64, 65], and enhance stress tolerance [37, 66]in plants, facilitating greater biomass and heavy metal uptake in contaminated environments. The interactions between *S. indica* and plant hosts such

as king grass [38, 39] and *Artemisia annua* L. [37] have been documented, highlighting increased accumulation capabilities for heavy metals such as Cd. However, the specific rhizosphere microbiota mechanisms underpinning these enhancements, particularly in hyperaccumulators like *S. alfredii*, remain poorly understood. We aimed to delve into the soil-plant-microbe interactions that contribute to improving the phytoremediation efficiency of hyperaccumulator *S. alfredii*.

3.1. *S. indica* colonization enhanced S uptake and growth of *S. alfredii* from soil

To assess the impact of *S. indica* on the phytoremediation efficiency of *S. alfredii*, we cultivated *S. alfredii* plants in Cd-contaminated soil under CK and +*Si* treatment. We observed the chlamydospores of *S. indica* were formed in the root after colonization (Fig. S1), suggesting the successful inoculation of *S. indica* in the root of *S. alfredii*. Earlier researchers found that *S. indica* improves nutrients uptake from soil and promotes plant growth [67]. We also found that shoot biomass was significantly improved by 211.32% under +*Si* treatment (Fig. 2a, b). *S. indica* employs diverse growth-promoting mechanisms, including regulating hormones [68, 69], enhancing tolerance [70], and facilitating nutrient acquisition [40, 44, 71]. In our study, *S. indica* enhanced plant growth through increasing plant S uptake (Fig. 4). Similarly, *SiSulT,* as a sulfate transporter of *S. indica* facilitates sulfate absorption by maize plants [40]. Furthermore, nano-XRF images showed that S hotspots were exhibited in the root and rhizoplane soil on the submicron scale under +*Si* treatment (Fig. 3b). A distinct distribution pattern of S on the rhizoplane, tightly encircling the roots. In contrast, under CK treatment, S showed an irregular distribution within the rhizosphere (Fig. 3a). This indicated that *S. indica* inoculation activated rhizosphere soil S, which promoted plants to uptake S from soil to the root. S is a critical component of glutathione and phytochelatins [72-75], which are essential for detoxification processes and chelating heavy metals such as Cd. To sum up, *S. indica* inoculation helped transport S to the plant.

Significant decreases were observed in the K localization of rhizosphere soil (Fig. 3). This depletion is a common response in plant-soil interactions. *S. indica* enhanced

plants' nutrient uptake capabilities [76, 77]. The symbiotic relationship with *S. indica* not only boosts K absorption due to increased metabolic needs and growth but also influences root architecture, promoting increased branching and thus expanding the root surface area for more effective nutrient extraction.

3.2. *S. indica* colonization facilitated Cd absorption and soil Cd mobilization

S. indica not only promoted plant growth but also facilitated Cd uptake by *S. alfredii*. In our study, although the Cd concentration showed no significant difference in the shoot under +*Si* treatment (Fig. 2c), the Cd accumulation increased by 235.72% remarkably in the shoot of *S. alfredii* (Fig. 2d). Cd influx reached 3.98 mg Cd·g^{-1} dry weight, which was 2.73-fold higher than that under CK treatment (Fig. 2e). Previous research also showed that *S. indica* increased Cd uptake by king grass [38]. Meanwhile, we also found that soil Cd concentrations decreased significantly by 32.17% in rhizosphere soils under +*Si* treatment (Table 1). Liu, et al. also found that endophyte led to a significant decrease of soil Cd concentration [78].

Moreover, TFs, BFs, and removal efficiency are used to gauge the phytoextraction potential of plants [79]. *S. indica* inoculation significantly promoted TFs, BFs and removal efficiency of Cd (Fig. 2f, g and h). The average TF value (7.58) under CK treatment was significantly lower than that (8.92) under +*Si* treatment. Higher TFs value indicated that *S. indica* can promote Cd transport from root to shoot. But previous researchers found that *S. indica* reduced the TFs of arsenic (As) and Cd in rice [80] and sunflower [36] by sequestering these heavy metals within the root systems. This is due to variations in heavy metal transport capacities among different plant species. Hyperaccumulator plants can transport heavy metals from root to shoot efficiently [13, 81-83]. *S. alfredii* is recognized as a hyperaccumulator plant celebrated for its high-efficiency mechanism of translocating nutrients from roots to shoots [13]. *S. alfredii* exhibited shoot Cd accumulation of 96.6 mg·kg^{-1}, with a corresponding BF of 29.5 in soils that harbored Cd at 0.90 mg·kg^{-1}. Meanwhile, it phytoextracted approximately 540 μg Cd over six months [84]. However, we found that the average BF exhibited a significant increase under +*Si* treatment. The average BF greatly reached 58.02, representing a substantial enhancement compared to CK treatment (Fig. 2g).

The BF was used to assess the ability of plants to transport or accumulate Cd from the soil into their shoots, revealing an enhanced BF in plants associated with *S. indica*. This increase is attributed to several factors: the fungus induces a larger root biomass and surface area, enhancing soil contact and Cd uptake [85, 86]; it alters the rhizosphere chemistry, increasing Cd solubility through reduced pH and the release of chelating agents [38]; and it stimulates the production of metal-binding proteins and phytochelatins that aid in Cd detoxification and accumulation [87, 88]. These findings highlight the potential of *S. indica* to not only enhance plant growth and stress tolerance but also improve phytoremediation efficiency in Cd-contaminated soils, offering valuable insights into the ecological and practical applications of using endophytic fungi in environmental pollution management. Furthermore, Cd accumulation in *S. alfredii* shoots impressively reached 593.15 μg in just 60 days under +*Si* treatment (Fig. 2d). During the remediation, the bioavailability of soil heavy metal determines the remediation efficiency [89]. *S. indica* directly increases root biomass by producing indole-3-acetic acid (IAA) and organic acid [65]. Due to the increase of organic acid, reduced rhizosphere soil pH could help Cd and S mobilization and absorption (Table 1 and Fig. 4c). Jiang, et al. also believed that important targets and signaling components of phytohormones in response to abiotic stress [90].

To explore *in situ* distribution of Cd in the root-soil interface under +*Si* treatment, high-resolution nano-XRF mapping was utilized on cross-sections of the root-soil interface. We found that *S. indica* inoculation significantly altered Cd distribution in the root-soil interface. Cd were preferentially located in the rhizosphere but less in the root under CK treatment (Fig. 3a). Under +*Si* treatment, Cd were preferentially allocated to the root and the rhizoplane, tightly encircling the roots with the highest intensity found within the rhizoplane (Fig. 3b). To better show the difference, images were digitally extracted and made into a composite for comparison (Fig. S5). Cd intensity values of the selected areas (marked with a white scanning lines of Fig. 3) across the root-soil interface (from L1 to L2) are shown. Nano-XRF mapping revealed that *S. indica* inoculation enhances the root system's ability to absorb Cd

353 from the soil. Prior researches also showed PGPM depends on the activation of soil
354 heavy metals to enhance phytoremediation [91, 92]. The bulk and rhizosphere soil pH
355 exhibited a significant decrease under +*Si* treatment (Table 1). The decrease of soil pH
356 contributes to an increased soil Cd availability and absorption by plant roots.
357 Moreover, S may improve the Cd availability of the rhizosphere soils in previous
358 researches [93, 94]. To explore the relationship between S and Cd, we extracted the
359 intensity values of Cd and S specifically from the rhizoplane of the Nano-XRF image
360 (Fig. 3) and conducted linear fitting. This analysis revealed a significant correlation
361 between Cd and S in both CK and +*Si* treatments (Fig. S6). Moreover, under +*Si*
362 treatment, the correlation was notably stronger. This indicates that S may facilitate the
363 soil Cd mobilization. Localized measurements at the root-soil interface are crucial for
364 capturing the true dynamics between these elements using Nano-XRF. Therefore, *S.*
365 *indica* enhances Cd accumulation in the host plant and augments phytoremediation
366 efficiency by promoting both plant biomass and Cd uptake from the soil. The *S.*
367 *indica*-*S. alfredii* mutualism systems have great potential in phytoremediation. The
368 systems facilitated Cd bioavailability of soil, Cd uptake, and Cd accumulation of
369 hyperaccumulator shoot.

370 **3.3. *S. indica* colonization recruited specific microbial taxa related to S cycle**

371 *S. indica* inoculation resulted in a remarkable increase of shoot biomass by 211.32%
372 in native soil (Fig. 2b). Conversely, in γ-irradiated soil, the improvement in shoot
373 biomass was comparatively lower, with only a 25.93% increase observed (Table S1).
374 These results suggested that soil microbial communities played a key role, consistent
375 with recent studies that strong correlations between root endophytic fungi and the
376 composition of soil microbial communities [95].

377 To delve deeper into the factors affecting rhizosphere microbial variation, we
378 conducted a Mantel analysis to assess the connection between microbial communities
379 and environmental variables (Fig. 4a). The assessment of the microbial communities
380 was performed using Mantel's p and Mantel's r. We found that the rhizosphere
381 communities were significantly affected by biomass, shoot S concentration, available
382 S concentration, organic matter concentration, soil total S concentration, and pH

under +*Si* treatment (Fig. 4a). Meanwhile, soil total S concentration and available S concentration in the rhizosphere were increased by 21.50% and 68.85%, respectively (see Fig. 4b and c). We also found that *S. indica* significantly enhanced the S concentration of the shoot (Fig. 4d).

Utilizing Faith's phylogenetic diversity index, a significant enhancement of both bacterial and fungal community diversities was showed in the rhizosphere under +*Si* treatment (Fig. 5a, Table S2). This increase in phylogenetic diversity does not correspond to changes in observed OTUs, Shannon index, or evenness, as these indices did not show significant differences between treatments (Table S2). This distinction highlights that the +*Si* treatment enriches the rhizosphere in more phylogenetically diverse taxa. The principal coordinates analysis (PCoA) illustrated a distinct segregation among the unplanted soil, bulk soil, and rhizosphere soil for both bacteria and fungi (Fig. 5b). But it seems like an unclear segregation between CK and +*Si* treatment groups (Fig. 5b). This aligns with previous findings that *S. indica* actively modulates the diversity of both bacteria and fungi in the rhizosphere soil [37]. When it comes to the microbial community composition, a diverse array of predominant bacterial species was identified, encompassing eight phyla, such as Proteobacteria, Bacteroidota, Actinobacteria, Chloroflexi, Acidobacteriota, Gemmatimonadetes, Myxococcota, and Verrucomicrobiota. In addition, the phyla of Ascomycota, Glomeromycota, and Basidiomycota were identified as the prevailing fungal species, accounting for most of the fungi present. A small proportion of ASVs (less than 5%) were categorized as Rozellomycota and Mortierellomycota (Fig. 5c).

DESeq2 analysis elucidated variations in ASV levels (Table S3). Fifteen core bacterial ASVs and two core fungal ASVs were identified in +*Si* treatment. The abundances of specific bacteria and fungi enriched significantly in the rhizosphere under +*Si* treatment (Fig. 5d, e, f, and g). These were identified as the dominant members of the rhizosphere microbiomes. As shown in Fig. 5h and i, the abundances of *Lacunisphaera*, Pedosphaeraceae, *Bradyrhizobium*, *Novosphingobium*, Comamonadaceae, and *Entoloma* (BASV1197, 1236, 890, 921, 964 and FASV213) displayed positive correlations with soil AvS and S concentration, plant biomass, and

shoot S concentration (blue arrow in Fig. 5h and i). In contrast, they exhibited a negative correlation with soil pH. *Bradyrhizobium* and *Novosphingobium* are involved in S oxidation [96, 97], and strengthen soil metabolic ability [98]. The Comamonadaceae family played a pivotal role in mineralization of carbon-bound S, transformation of soil sulfate between organic and inorganic states [99]. S desulfonation reactions that provide an important source of S for wheat from soil [100].

Moreover, the keystone microbial taxa were related to plant growth promotion and Cd tolerance under +*Si* treatment (Fig. 5h and i), such as Pedosphaeraceae and *Bradyrhizobium*. Pedosphaeraceae is a metabolic generalist with vital ecological functions. It can promote plant growth and tolerate Cd bio-toxicity [101, 102]. *Bradyrhizobium* is not only endophytic in rice plants and contributes to improving crop yield [103, 104], but also directly participates in reducing the oxidative damage of Cd [105]. It is regarded as a potential bacterial resource for maintaining community stability and Cd contamination bioremediation [106]. Further, we also found that *Piscinibacter* and *Entoloma* were related to soil acidification (Fig. 5e), which is the first time to be reported. These specific microbiomes could be potential microbial regulators for the optimization of Cd-contaminated phytoremediation. We concluded that *S. indica* could recruit specific microbiomes related to the S cycle, growth promotion, and Cd uptake of plant, thereby reshaping rhizosphere microecology. The rhizosphere microecology could promote S absorption, plant growth, soil Cd mobilization, and phytoremediation efficiency.

3.4. *S. indica* inoculation greatly alters microbial community network topologies

Not only is it important to decipher the keystone taxa, but the network hubs correlated with the *S. indica* and host plants are vital for utilizing plant microbiota to boost plant growth and health [107, 108]. Network analyses of MENs were performed to unveil the microbial interactions within the bacterial and fungal communities, elucidating distinct topological characteristics (Table S4 and Fig. 6a). We depicted microbial interactions with microbial ecological networks in both the CK and +*Si* treatment (Fig. 6a). Network analysis was utilized to acquire co-occurrence patterns between bacteria and fungi. The modularity threshold exceeded 0.4 (Table S4), thus signifying a typical

module structure [109, 110]. The values of edge numbers, average degree (avgK), average clustering coefficient (avgCC), and modularity in empirical networks under +*Si* treatment were higher than those under CK treatment (Table S4), representing greater complexity and connectivity [62, 111]. Previous research also showed that beneficial fungi generate positive feedbacks [112], The positive feedbacks enhance their competitiveness and interactions with neighbors to alter microbial community structures [113]. Therefore, *S. indica* inoculation shaped more steady microbial networks of soil.

Stable microbial networks can provide a favorable environment for shoot and root development to optimize nutrient cycling and transformation processes [114, 115]. Under +*Si* treatment, Module 1 was highly correlated with plant biomass, shoot S concentration, and AvS, while Module 4 was correlated with soil available Cd (Fig. 6b). Comamonadaceae (class Gammaproteobacteria) of Modules 1 commonly inhabit the rhizosphere soils of terrestrial plants, which promote plant growth [116]. Moreover, they are closely related to the citric acid cycle. The hydrogen ions (H^+) in the citric acid cycle decreased soil pH significantly, regulating soil properties and the microbial community networks [117]. Decreased soil pH facilitated heavy metals and S mobilization. Moreover, Comamonadaceae is involved in desulfonation reactions [100], potentially providing S source of plant nutrition in the rhizosphere of *S. alfredii*. In addition, Sphingomonadaceae (class Alphaproteobacteria) of Module 4 was found in the rhizosphere. Sphingomonadaceae can produce and release ACC deaminase, IAA, and siderophores. These contribute to root elongation and heavy metal tolerance of plants [118, 119], resulting in greater plant biomass and Cd accumulation. Environmental functional modules played direct or indirect roles in activating and facilitating S and Cd uptake by roots, thereby fostering plant growth and Cd accumulation. The rhizosphere soil microbial networks exhibited robust correlations with the phytoextraction potential of plant nutrients under +*Si* treatment. PLS-PM analysis also extensively elucidated how different factor strategies influenced both the rhizosphere microbial ecology and Cd remediation efficiency from the soil (Fig. S4). The model exhibited a good fit to the data, with a goodness-of-fit (GoF) value of 0.82.

S. indica treatment directly affected soil pH, soil available S concentration, rhizosphere microbial communities, and Cd remediation efficiency. The Cd remediation efficiency was indirectly influenced by rhizosphere microbial communities. Therefore, reshaped microbial community networks synergistically could promote plant growth and enhanced the accumulation of heavy metals in the shoot.

In conclusion, we successfully visualized the submicron-scale spatial distribution of key elements at the root-soil interface induced by *S. indica* inoculation using Nano-XRF for the first time. *S. indica* can colonize *S. alfredii* roots and recruit specific microbial taxa related with plant growth promotion and nutrient and heavy metal mobilizations in the rhizosphere. *S. indica* could help plants thrive and increase Cd accumulation in plants, having potential of endophyte-assisted phytoremediation to regulate microecology characteristics and its promising application in sustainable agriculture. In the future, we will focus on the cellular-level distribution of elements, metabolomics, and metagenomic analysis to further elucidate the interaction between microbes, plants, and rhizosphere processes of heavy metals in contaminated farmland.

Author information

Corresponding Author

Shengke Tian - *MOE Key Laboratory of Environment Remediation and Ecological Health, College of Environmental & Resource Science, Zhejiang University, Hangzhou 310058, P.R. China; Zhejiang Provincial Key Laboratory of Subtropic Soil and Plant Nutrition, Zhejiang University, Hangzhou 310058, P.R. China;* orcid.org/0000-0001-8242-3581; Phone: 86-15700123781; E-mail: tiansk@zju.edu.cn.

Authors

Yabei Qiao - *MOE Key Laboratory of Environment Remediation and Ecological Health, College of Environmental & Resource Science, Zhejiang University, Hangzhou 310058, P.R. China; Zhejiang Provincial Key Laboratory of Subtropic*

Soil and Plant Nutrition, Zhejiang University, Hangzhou 310058, P.R. China; orcid.org/0000-0002-1529-0392

Zhi Lin - *MOE Key Laboratory of Environment Remediation and Ecological Health, College of Environmental & Resource Science, Zhejiang University, Hangzhou 310058, P.R. China; Zhejiang Provincial Key Laboratory of Subtropic Soil and Plant Nutrition, Zhejiang University, Hangzhou 310058, P.R. China.*

Luxi Li – *Advanced Photon Source, Argonne National Laboratory, Lemont, Illinois 60439, USA.*

Wei Jiang - *Xianghu Laboratory, Biotechnology Institute, Hangzhou 311231, P.R. China.*

Jun Ge - *MOE Key Laboratory of Environment Remediation and Ecological Health, College of Environmental & Resource Science, Zhejiang University, Hangzhou 310058, P.R. China; Zhejiang Provincial Key Laboratory of Subtropic Soil and Plant Nutrition, Zhejiang University, Hangzhou 310058, P.R. China.*

Jiuzhou Chen - *MOE Key Laboratory of Environment Remediation and Ecological Health, College of Environmental & Resource Science, Zhejiang University, Hangzhou 310058, P.R. China; Zhejiang Provincial Key Laboratory of Subtropic Soil and Plant Nutrition, Zhejiang University, Hangzhou 310058, P.R. China.*

Lingli Lu - *MOE Key Laboratory of Environment Remediation and Ecological Health, College of Environmental & Resource Science, Zhejiang University, Hangzhou 310058, P.R. China; Zhejiang Provincial Key Laboratory of Subtropic Soil and Plant Nutrition, Zhejiang University, Hangzhou 310058, P.R. China.*

Supporting Information

Supplemental methods and additional results. Dry biomass and Cd concentration of *S. alfredii* **(Table S1)**; microbial α-diversity **(Table S2)**; differential ASVs assessed by DESeq2 **(Table S3)**; topological properties of networks **(Table S4)**; soil microbial community composition **(Table S5)**; microscopy of *S. indica* chlamydospores **(Fig. S1)**; Cd, K, and S distribution in root-soil interface **(Fig. S2)**; Z-P plot of ASVs **(Fig. S3)**; PLS-PM analysis **(Fig. S4)**; Cd intensity of the selected areas **(Fig. S5)**; correlation between Cd vs S intensities **(Fig. S6)**.

Notes

The authors declare no competing financial interest.

Acknowledgments

This work has been funded by the National Natural Science Foundation of China (grant number 42377021), the Natural Science Foundation of Zhejiang Province (grant number LZ22D010004), the National Key Research and Development Program of China (grant numbers 2023YFC3706700), the National Natural Science Foundation of China (grant number 41977130), and the Department of Science and Technology of Zhejiang Province (grant number 2023C02002).This research used resources of the Advanced Photon Source, a U.S. Department of Energy (DOE) Office of Science user facility operated for the DOE Office of Science by Argonne National Laboratory under Contract No. DE-AC02-06CH11357.

Abbreviations

As, arsenic; avgK, average degree; ASVs, amplicon sequence variants; avgCC, average clustering coefficient; BF, bioaccumulation factor; Cd, cadmium; DOC, dissolved organic carbon; DON, dissolved organic nitrogen; Faith_pd, faith's phylogenetic diversity index; IAA, indole-3-acetic acid; LSD, least significant difference; MENA, molecular ecological network analysis pipeline; MENs, molecular ecological networks; Nano-XRF, Nano x-ray fluorescence; OM, soil organic matter; K, potassium; P, phosphorus; PCoA, principal coordinates analysis; PGPM, plant-growth-promoting microorganisms; Pi, among-module connectivity; PLS-PM, partial least squares path modeling; QIIME2, Quantitative Insights into Microbial Ecology 2; RMT, random matrix theory; S, sulfur; *S. alfredii, Sedum alfredii* Hance; *S. indica, Serendipita indica*; SOM, soil organic matter; SR-XRF, synchrotron-based x-ray fluorescence; TF, translocation factor; Un, unplanted; Zi, within-module connectivity

Figure and Table Captions

Table 1 Soil physicochemical parameters under CK and +*Si* treatments. The mean values (with corresponding standard deviations) were calculated (n = 6). Significance levels at $p < 0.05$, $p < 0.01$, and $p < 0.001$ were denoted with *, **, and ***, respectively, using the student's t-test to identify significant differences between treatments. DOC: dissolved organic carbon, DON: dissolved organic nitrogen, TCd: total cadmium concentration, AvCd: available Cd concentration. CK, without *S. indica* inoculation treatment; +*Si*, with *S. indica* inoculation treatment.

Fig. 1 Schematic illustration of the experimental procedures. (a) The root bag system, containing the bulk and rhizosphere compartments; (b) Seedlings are transplanted into soil of the root bags; (c) Desired input *S. indica* is inoculated using a 1 mL pipette and pots are transferred to the greenhouse; (d) Sample collection and determination by high-throughput sequencing and Nano-XRF imaging.

Fig. 2 *S. indica* promotes plant growth in Cd contaminated soil. (a) Growth status of *S. alfredii* planted in Cd contaminated soil without *S. indica* (CK) and with *S. indica* inoculation treatment (+*Si*). Dry biomass ($g \cdot plant^{-1}$) (b), Cd concentration (c), Cd accumulation (d), Cd influx (e), translocation factors (f), bioaccumulation factors (g), and Cd removal efficiency (h) in *S. alfredii*. The asterisks *, **, and *** represent significant differences between CK and +*Si* treatment at $p < 0.05$, $p < 0.01$, and $p < 0.001$, respectively. Scale bars = 5 cm.

Fig. 3 Nano-XRF mapping of elements (Cd, K, and S) in the cross-sections of root-soil interface collected from CK (a) and +*Si* (b) treatment. Pixel brightness is displayed in RGB. Fluorescence intensities ($\mu g \cdot cm^{-2}$) of elements Cd, K, and S were normalized and scaled between red (high) and blue (low) for each map. Bar = 200 μm. CK, without *S. indica* inoculation treatment; +*Si*, with *S. indica* inoculation treatment.

Fig. 4 Drivers of variation in the rhizosphere microbiota. (a) Mantel analysis maps showed the relationship between environmental physicochemical properties and the composition of microbial communities under without *S. indica* (CK) and with *S. indica* inoculation treatment (+*Si*). Soil sulfur concentration (b), soil available sulfur

concentration (c), and sulfur concentration in plant (d) are showed. Asterisks indicate values that are significantly different from CK and +*Si* treatment (*$p < 0.05$, **$p < 0.01$, ***$p < 0.001$). The letters a and b indicate significant differences between bulk and rhizosphere at $p < 0.05$ under CK treatment. The letters a' and b' indicate significant differences between bulk and rhizosphere at $p < 0.05$ under +*Si* treatment. Cd: soil Cd concentration, S: soil sulfur concentration, AvCd: soil available Cd concentration, AvS: soil available sulfur concentration, DOC: soil dissolved organic carbon, DON: soil dissolved organic nitrogen, OM: soil organic matter. CK, without *S. indica* inoculation treatment; +*Si*, with *S. indica* inoculation treatment.

Fig. 5 Assembly of bacterial and fungal communities in the bulk and rhizosphere soil and Spearman correlation analysis of keystone ASVs with rhizosphere soil and plant properties. (a) Box plots for alpha-diversity indices, including the faith's phylogenetic diversity of bacterial and fungal communities in rhizosphere and root under without *S. indica* (CK) and with *S. indica* inoculation treatment (+*Si*). The asterisks *, **, and *** represent significant differences between CK and *S. indica* inoculation treatment at $p < 0.05$, $p < 0.01$, and $p < 0.001$, respectively. (b) Principal coordinate analysis (PCoA) plots for visualizing the Bray-Curtis dissimilarity matrix among the bacterial communities and fungal communities. (c) Relative abundances of bacterial and fungal communities in rhizosphere soils of *S. alfredii* grown in Cd contaminated soil without *S. indica* (CK) and with *S. indica* inoculation treatment (+*Si*). Keystone ASVs used for discriminating bacterial (d) and fungal (e) communities without *S. indica* (CK) and with *S. indica* inoculation treatment (+*Si*) (detected by random forest model). The assigned taxonomy of each taxon is displayed at the ASV level. The bubbles show the ASVs numbers of bacteria (f) and fungi (g) without *S. indica* (CK) and with *S. indica* inoculation treatment (+*Si*); the Spearman correlations between environmental variables and the relative abundances of keystone ASVs are depicted in the right heatmaps (h and i). Cd, soil Cd concentration; S, soil sulfur concentration; AvCd, soil available Cd concentration; AvS, soil available sulfur concentration; DOC, soil dissolved organic carbon; DON, soil dissolved organic nitrogen; OM, soil organic matter. *$p < 0.05$, **$p < 0.01$, ***$p < 0.001$.

Fig. 6 Microbial ecology networks and functional modules of *S. alfredii* rhizosphere bacteria and fungi, and their relationships with environmental factors. (a) Networks contained both bacterial and fungal taxa, showing a higher number of edges in the *S. indica* inoculation treatment than those in CK networks. The nodes are colored according to bacterial and fungal phylum. The edge color represents positive (blue) and negative (purple) correlations. (b) Spearman's correlation analysis of modules with rhizosphere soil and plant properties in CK and *S. indica* inoculation treatment. Only significant correlations ($p < 0.05$) are shown. Cd, soil Cd concentration; S, soil sulfur concentration; AvCd, soil available Cd concentration; AvS, soil available sulfur concentration; DOC, soil dissolved organic carbon; DON, soil dissolved organic nitrogen; OM, soil organic matter. *$p < 0.05$, **$p < 0.01$, ***$p < 0.001$. CK, without *S. indica* inoculation treatment; +*Si*, with *S. indica* inoculation treatment.

Table 1 Soil physicochemical parameters under CK and +*Si* treatments.

	DOC ($mg \cdot L^{-1}$)	DON ($\mu g \cdot L^{-1}$)	pH	TCd ($mg \cdot kg^{-1}$)	AvCd (($mg \cdot kg^{-1}$)
Bulk					
CK	81.71 ± 2.45	12431.00 ± 1554.10 **	6.83 ± 0.02 *	5.81 ± 0.11 ***	2.47 ± 0.04 ***
+Si	78.67± 2.69	8234.78 ± 491.37	6.78 ± 0.02	4.93 ± 0.20	1.83 ± 0.08
Rhizosphere					
CK	99.23 ± 1.93	16220.56 ± 1485.53 ***	6.72 ± 0.01 ***	4.93 ± 0.10 ***	2.00 ± 0.06 ***
+Si	95.45 ± 2.78	9748.85 ± 490.13	6.63 ± 0.01	3.73 ± 0.17	1.52 ± 0.07

The mean values (with corresponding standard deviations) were calculated (n = 6). Significance levels at $p < 0.05$, $p < 0.01$, and $p < 0.001$ were denoted with *, **, and ***, respectively, using the student's t-test to identify significant differences between treatments. DOC: dissolved organic carbon, DON: dissolved organic nitrogen, TCd: total cadmium concentration, AvCd: available Cd concentration. CK, without *S. indica* inoculation treatment; +*Si*, with *S. indica* inoculation treatment.

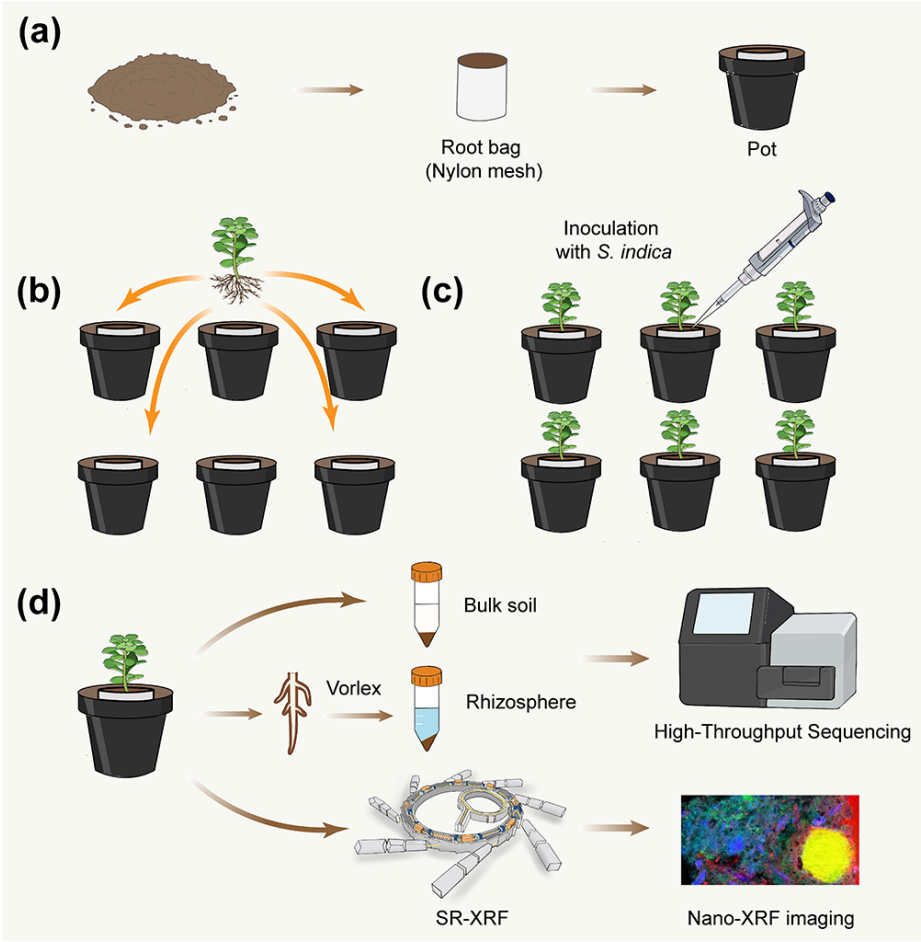

637

638 **Fig. 1** Schematic illustration of the experimental procedures. (a) The root bag system,
639 containing the bulk and rhizosphere compartments; (b) Seedlings are transplanted into
640 soil of the root bags; (c) Desired input *S. indica* is inoculated using a 1 mL pipette and
641 pots are transferred to the greenhouse; (d) Sample collection and determination by
642 high-throughput sequencing and Nano-XRF imaging.

643

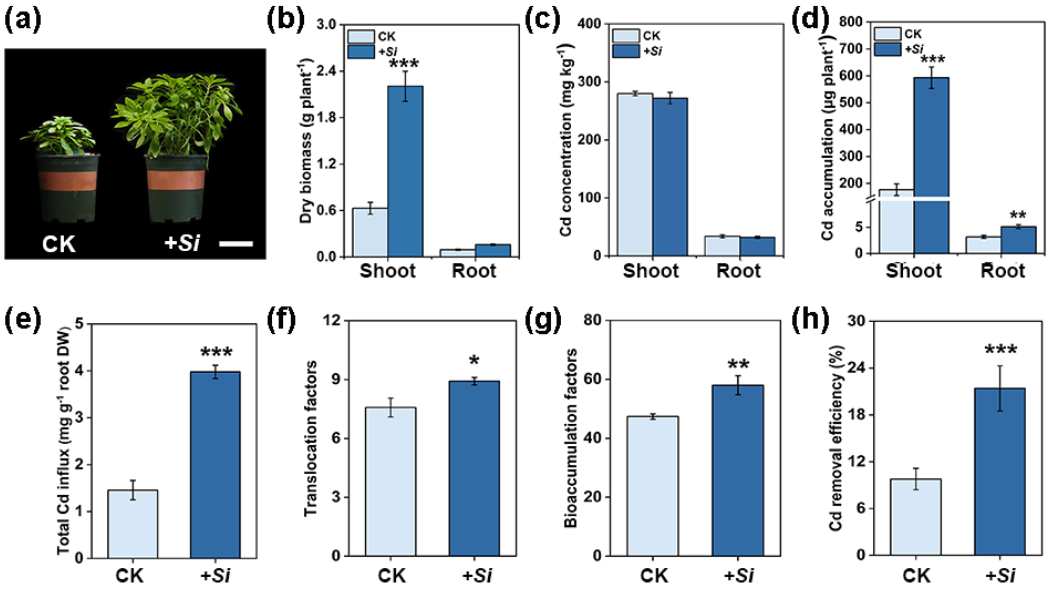

Fig. 2 *S. indica* promotes plant growth in Cd contaminated soil. (a) Growth status of *S. alfredii* planted in Cd contaminated soil without *S. indica* (CK) and with *S. indica* inoculation treatment (+*Si*). Dry biomass (g·plant^{-1}) (b), Cd concentration (c), Cd accumulation (d), Cd influx (e), translocation factors (f), bioaccumulation factors (g), and Cd removal efficiency (h) in *S. alfredii*. The asterisks *, **, and *** represent significant differences between CK and +*Si* treatment at $p < 0.05$, $p < 0.01$, and $p < 0.001$, respectively. Scale bars = 5 cm.

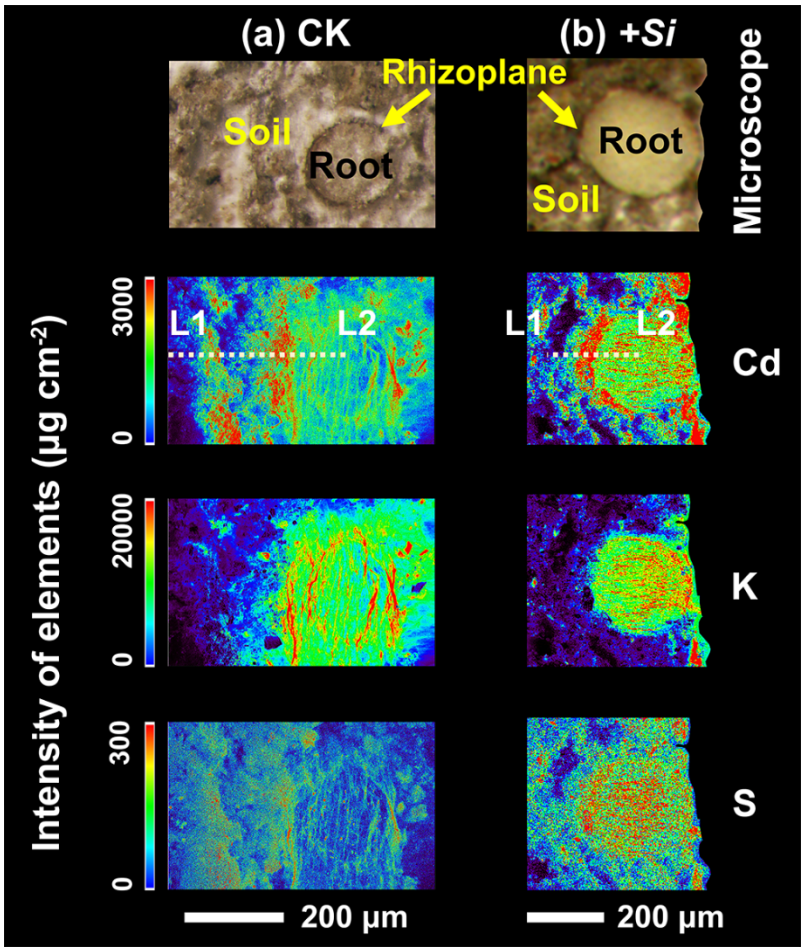

652

653 **Fig. 3** Nano-XRF mapping of elements (Cd, K, and S) in the cross-sections of
654 root-soil interface collected from CK (a) and +*Si* (b) treatment. Pixel brightness is
655 displayed in RGB. Fluorescence intensities (μg·cm^{-2}) of elements Cd, K, and S were
656 normalized and scaled between red (high) and blue (low) for each map. Bar = 200 μm.
657 CK, without *S. indica* inoculation treatment; +*Si*, with *S. indica* inoculation treatment.

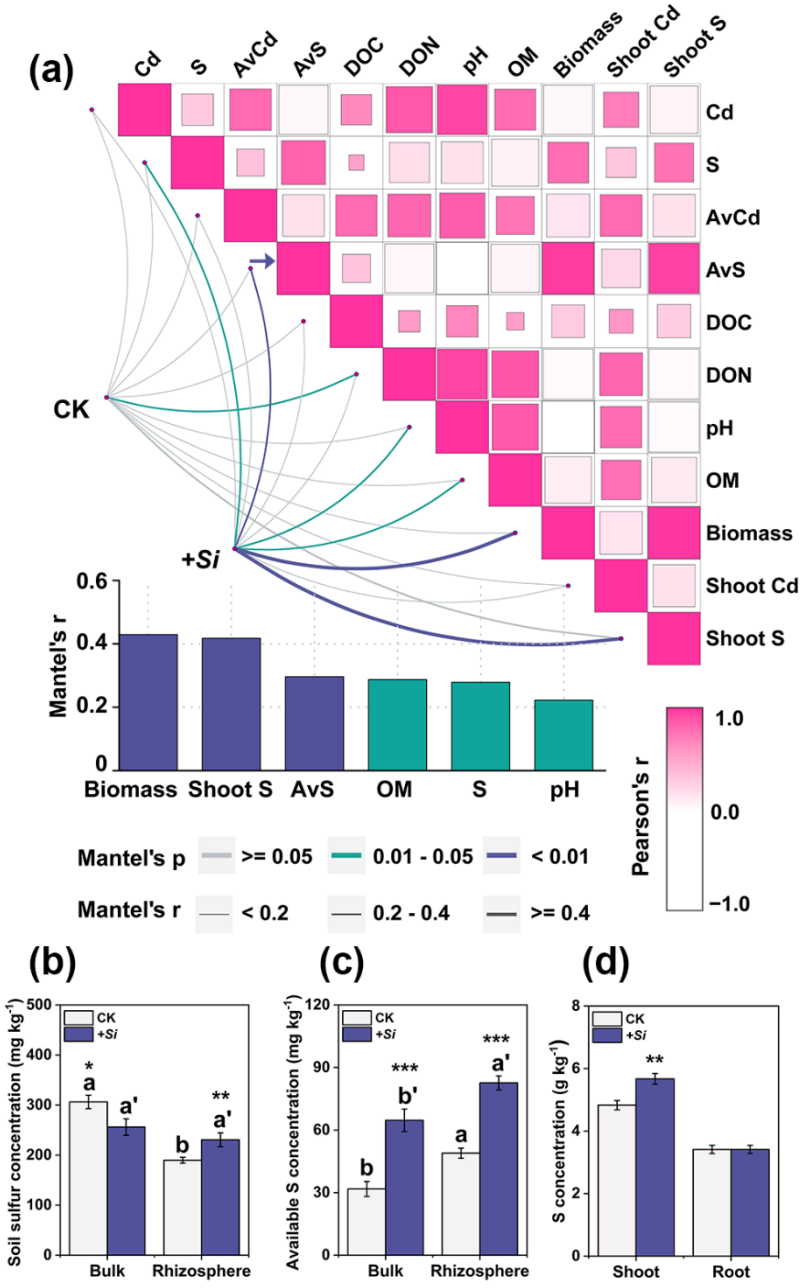

Fig. 4 Drivers of variation in the rhizosphere microbiota. (a) Mantel analysis maps showed the relationship between environmental physicochemical properties and the composition of microbial communities under without *S. indica* (CK) and with *S. indica* inoculation treatment (+*Si*). Soil sulfur concentration (b), soil available sulfur concentration (c), and sulfur concentration in plant (d) are showed. Asterisks indicate values that are significantly different from CK and +*Si* treatment (*$p < 0.05$, **$p < 0.01$, ***$p < 0.001$). The letters a and b indicate significant differences between bulk and rhizosphere at $p < 0.05$ under CK treatment. The letters a' and b' indicate

667 significant differences between bulk and rhizosphere at $p < 0.05$ under *+Si* treatment.
668 Cd: soil Cd concentration, S: soil sulfur concentration, AvCd: soil available Cd
669 concentration, AvS: soil available sulfur concentration, DOC: soil dissolved organic
670 carbon, DON: soil dissolved organic nitrogen, OM: soil organic matter. CK, without *S.*
671 *indica* inoculation treatment; *+Si*, with *S. indica* inoculation treatment.

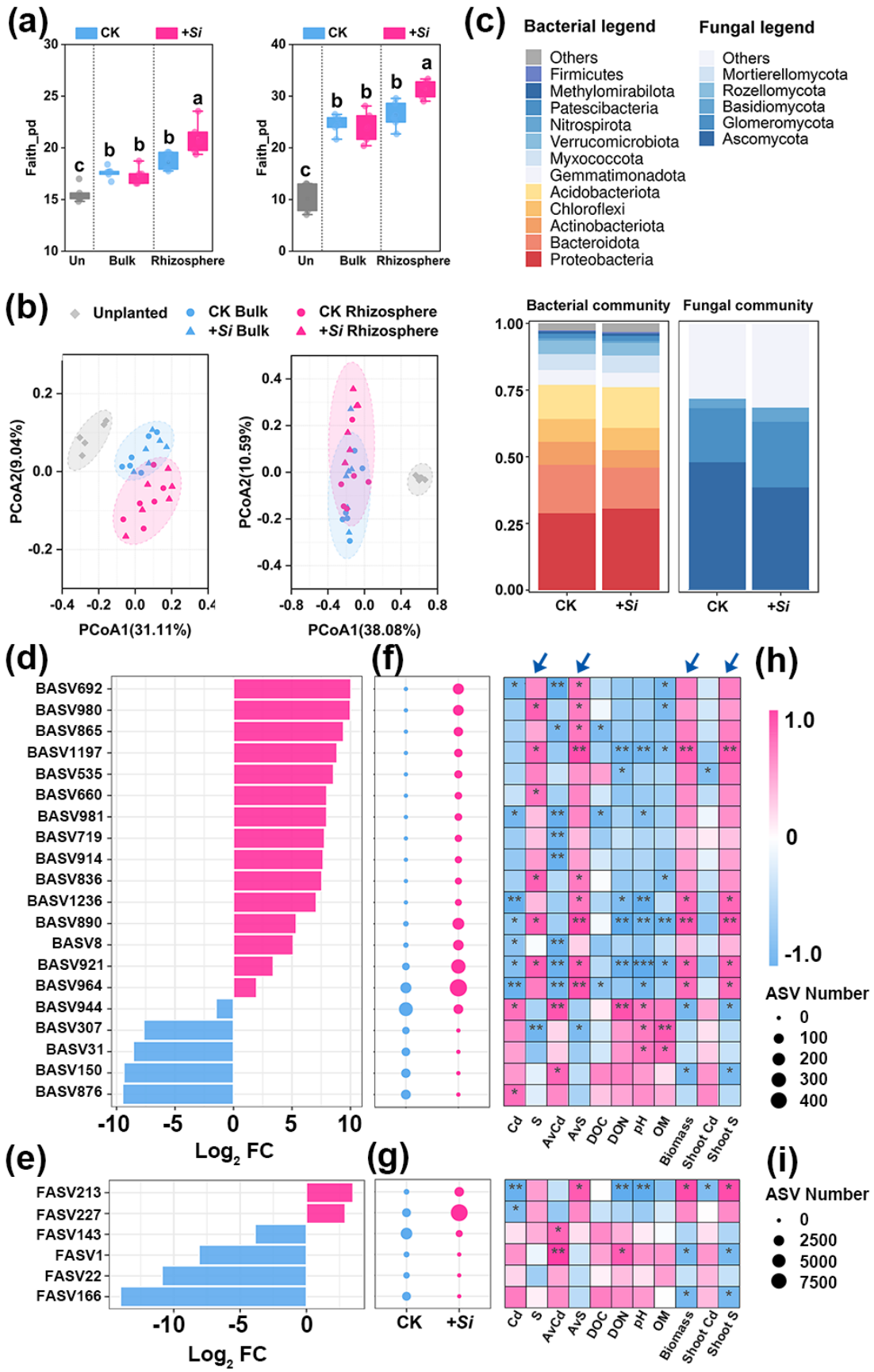

672

673 **Fig. 5** Assembly of bacterial and fungal communities in the bulk and rhizosphere soil

674 and spearman correlation analysis of keystone ASVs with rhizosphere soil and plant

properties. (a) Box plots for alpha-diversity indices, including the faith's phylogenetic diversity of bacterial and fungal communities in rhizosphere and root under without *S. indica* (CK) and with *S. indica* inoculation treatment (+*Si*). The asterisks *, **, and *** represent significant differences between CK and *S. indica* inoculation treatment at $p < 0.05$, $p < 0.01$, and $p < 0.001$, respectively. (b) Principal coordinate analysis (PCoA) plots for visualizing the Bray-Curtis dissimilarity matrix among the bacterial communities and fungal communities. (c) Relative abundances of bacterial and fungal communities in rhizosphere soils of *S. alfredii* grown in Cd-contaminated soil without *S. indica* (CK) and with *S. indica* inoculation treatment (+*Si*). Keystone ASVs used for discriminating bacterial (d) and fungal (e) communities without *S. indica* (CK) and with *S. indica* inoculation treatment (+*Si*) (detected by random forest model). The assigned taxonomy of each taxon is displayed at the ASV level. The bubbles show the ASVs numbers of bacteria (f) and fungi (g) without *S. indica* (CK) and with *S. indica* inoculation treatment (+*Si*); the Spearman correlations between environmental variables and the relative abundances of keystone ASVs are depicted in the right heatmaps (h and i). Cd, soil Cd concentration; S, soil sulfur concentration; AvCd, soil available Cd concentration; AvS, soil available sulfur concentration; DOC, soil dissolved organic carbon; DON, soil dissolved organic nitrogen; OM, soil organic matter. *$p < 0.05$, **$p < 0.01$, ***$p < 0.001$.

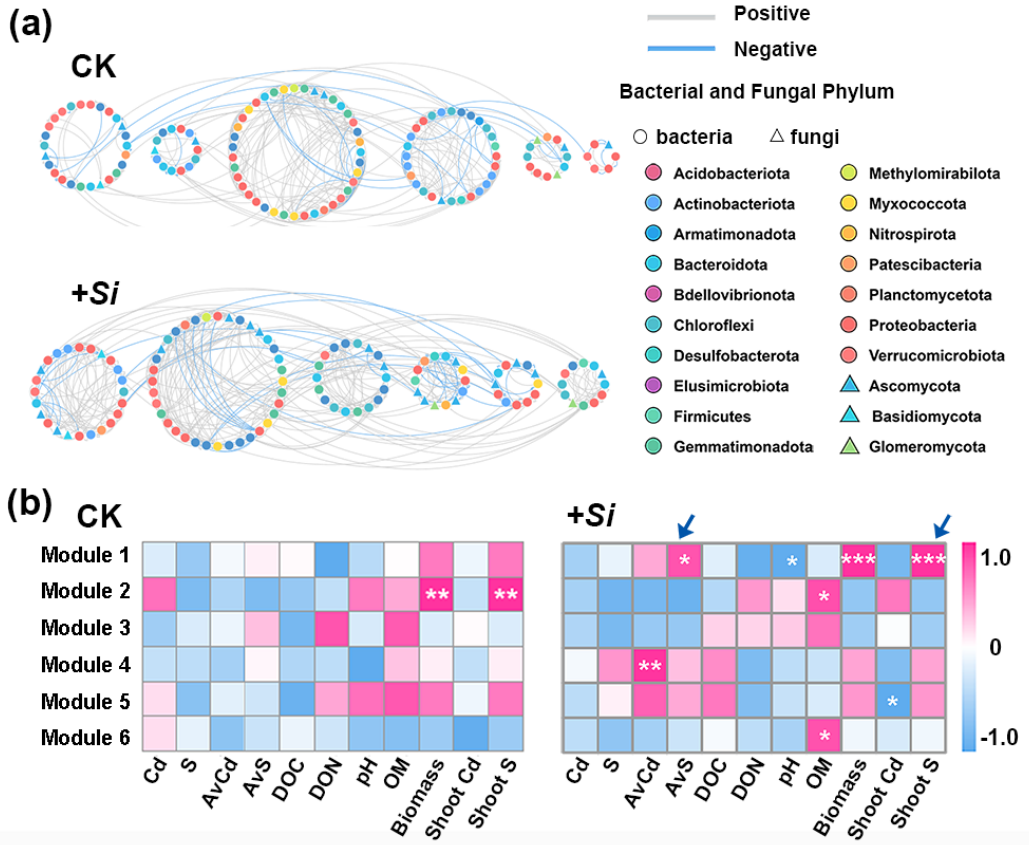

694

695 **Fig. 6** Microbial ecology networks and functional modules of *S. alfredii* rhizosphere
696 bacteria and fungi, and their relationships with environmental factors. (a) Networks
697 contained both bacterial and fungal taxa, showing a higher number of edges in the *S.*
698 *indica* inoculation treatment than those in CK networks. The nodes are colored
699 according to bacterial and fungal phylum. The edge color represents positive (blue)
700 and negative (purple) correlations. (b) Spearman's correlation analysis of modules
701 with rhizosphere soil and plant properties in CK and *S. indica* inoculation treatment.
702 Only significant correlations ($p < 0.05$) are shown. Cd, soil Cd concentration; S, soil
703 sulfur concentration; AvCd, soil available Cd concentration; AvS, soil available sulfur
704 concentration; DOC, soil dissolved organic carbon; DON, soil dissolved organic
705 nitrogen; OM, soil organic matter. *$p < 0.05$, **$p < 0.01$, ***$p < 0.001$. CK, without *S.*
706 *indica* inoculation treatment; *+Si*, with *S. indica* inoculation treatment.

Reference

1. Clemens, S.; Ma, J. F., Toxic heavy metal and metalloid accumulation in crop plants and foods. *Annual Review of Plant Biology* **2016,** *67*, 489-512.
2. Yang, J.; Hu, R.; Zhao, C.; Wang, L.; Lei, M.; Guo, G.; Shi, H.; Liao, X.; Chen, T., Challenges and opportunities for improving the environmental quality of cadmium-contaminated soil in China. *Journal of Hazardous Materials* **2023,** *445*, 130560.
3. Jiang, X.; Dai, J.; Zhang, X.; Wu, H.; Tong, J.; Shi, J.; Fang, W., Enhanced Cd efflux capacity and physiological stress resistance: the beneficial modulations of *Metarhizium robertsii* on plants under cadmium stress. *Journal of Hazardous Materials* **2022,** *437*, 129429.
4. Horiguchi, H.; Teranishi, H.; Niiya, K.; Aoshima, K.; Katoh, T.; Sakuragawa, N.; Kasuya, M., Hypoproduction of erythropoietin contributes to anemia in chronic cadmium intoxication: clinical study on Itai-itai disease in Japan. *Archives of Toxicology* **1994,** *68*, (10), 632-6.
5. Nordberg, G. F.; Nogawa, K.; Nordberg, M.; Friberg, L. T., Cadmium. In *Handbook on the Toxicology of Metals*, 2007; pp 445-486.
6. Pilon-Smits, E., Phytoremediation. *Annual Review of Plant Biology* **2005,** *56*, 15-39.
7. Jin, Y.; Wang, L.; Song, Y.; Zhu, J.; Qin, M.; Wu, L.; Hu, P.; Li, F.; Fang, L.; Chen, C.; Hou, D., Integrated life cycle assessment for sustainable remediation of contaminated agricultural soil in China. *Environmental Science & Technology* **2021,** *55*, (17), 12032-12042.
8. Wang, L.; Rinklebe, J.; Tack, F. M. G.; Hou, D., A review of green remediation strategies for heavy metal contaminated soil. *Soil Use and Management* **2021,** *37*, (4), 936-963.
9. Gavrilescu, M., Enhancing phytoremediation of soils polluted with heavy metals. *Current Opinion in Biotechnology* **2022,** *74*, 21-31.
10. Wood, J. L.; Tang, C.; Franks, A. E., Microbial associated plant growth and heavy metal accumulation to improve phytoextraction of contaminated soils. *Soil Biology and Biochemistry* **2016,** *103*, 131-137.
11. Yang, X.; Long, X.; Ye, H.; He, Z.; Calvert, D. V.; Stoffella, P. J., Cadmium tolerance and hyperaccumulation in a new Zn-hyperaccumulating plant species (*Sedum alfredii* Hance). *Plant and Soil* **2004,** *259*, (1/2), 181-189.
12. Cao, X.; Wang, X.; Lu, M.; Hamid, Y.; Lin, Q.; Liu, X.; Li, T.; Liu, G.; He, Z.; Yang, X., The Cd phytoextraction potential of hyperaccumulator *Sedum alfredii*-oilseed rape intercropping system under different soil types and comprehensive benefits evaluation under field conditions. *Environmental Pollution* **2021,** *285*, 117504.
13. Lu, L.; Tian, S.; Yang, X.; Wang, X.; Brown, P.; Li, T.; He, Z., Enhanced root-to-shoot translocation of cadmium in the hyperaccumulating ecotype of *Sedum alfredii*. *Journal of Experimental Botany* **2008,** *59*, (11), 3203-3213.
14. Tian, S.; Xie, R.; Wang, H.; Hu, Y.; Hou, D.; Liao, X.; Brown, P. H.; Yang, H.; Lin, X.; Labavitch, J. M.; Lu, L., Uptake, sequestration and tolerance of cadmium at cellular levels in the hyperaccumulator plant species *Sedum alfredii*. *Journal of Experimental Botany* **2017,** *68*, (9), 2387-2398.
15. Rajkumar, M.; Ae, N.; Freitas, H., Endophytic bacteria and their potential to enhance heavy metal phytoextraction. *Chemosphere* **2009,** *77*, (2), 153-60.
16. Sessitsch, A.; Kuffner, M.; Kidd, P.; Vangronsveld, J.; Wenzel, W. W.; Fallmann, K.; Puschenreiter, M., The role of plant-associated bacteria in the mobilization and phytoextraction of trace elements in contaminated soils. *Soil Biology and Biochemistry* **2013,**

751 *60*, 182-194.
752 17. Riaz, M.; Kamran, M.; Fang, Y.; Wang, Q.; Cao, H.; Yang, G.; Deng, L.; Wang, Y.; Zhou,
753 Y.; Anastopoulos, I.; Wang, X., Arbuscular mycorrhizal fungi-induced mitigation of heavy
754 metal phytotoxicity in metal contaminated soils: a critical review. *Journal of Hazardous*
755 *Materials* **2021,** *402*, 123919.
756 18. Ma, Y.; Rajkumar, M.; Moreno, A.; Zhang, C.; Freitas, H., Serpentine endophytic
757 bacterium *Pseudomonas azotoformans* ASS1 accelerates phytoremediation of soil metals
758 under drought stress. *Chemosphere* **2017,** *185*, 75-85.
759 19. Dimkpa, C.; Weinand, T.; Asch, F., Plant-rhizobacteria interactions alleviate abiotic stress
760 conditions. *Plant Cell And Environment* **2009,** *32*, (12), 1682-94.
761 20. Sarwar, N.; Imran, M.; Shaheen, M. R.; Ishaque, W.; Kamran, M. A.; Matloob, A.; Rehim,
762 A.; Hussain, S., Phytoremediation strategies for soils contaminated with heavy metals:
763 modifications and future perspectives. *Chemosphere* **2017,** *171*, 710-721.
764 21. Ji, S. H.; Gururani, M. A.; Chun, S. C., Isolation and characterization of plant growth
765 promoting endophytic diazotrophic bacteria from Korean rice cultivars. *Microbiological*
766 *Research* **2014,** *169*, (1), 83-98.
767 22. Liu, C.; Lin, H.; Li, B.; Dong, Y.; Gueret Yadiberet Menzembere, E. R., Endophyte
768 *Pseudomonas putida* enhanced *Trifolium repens* L. growth and heavy metal uptake: a
769 promising in-situ non-soil cover phytoremediation method of nonferrous metallic tailing.
770 *Chemosphere* **2021,** *272*, 129816.
771 23. Ma, Y.; Prasad, M. N.; Rajkumar, M.; Freitas, H., Plant growth promoting rhizobacteria
772 and endophytes accelerate phytoremediation of metalliferous soils. *Biotechnology Advances*
773 **2011,** *29*, (2), 248-58.
774 24. Wang, L.; Lin, H.; Dong, Y.; Li, B.; He, Y., Effects of endophytes inoculation on
775 rhizosphere and endosphere microecology of Indian mustard (*Brassica juncea*) grown in
776 vanadium-contaminated soil and its enhancement on phytoremediation. *Chemosphere* **2020,**
777 *240*, 124891.
778 25. Sheng, X.; He, L.; Wang, Q.; Ye, H.; Jiang, C., Effects of inoculation of
779 biosurfactant-producing *Bacillus* sp. J119 on plant growth and cadmium uptake in a
780 cadmium-amended soil. *Journal of Hazardous Materials* **2008,** *155*, (1-2), 17-22.
781 26. Hou, D.; Wang, K.; Liu, T.; Wang, H.; Lin, Z.; Qian, J.; Lu, L.; Tian, S., Unique
782 rhizosphere micro-characteristics facilitate phytoextraction of multiple metals in soil by the
783 hyperaccumulating plant *Sedum alfredii*. *Environmental Science & Technology* **2017,** *51*, (10),
784 5675-5684.
785 27. Luo, J.; Liu, Y.; Tao, Q.; Hou, Q.; Wu, K.; Song, Y.; Liu, Y.; Guo, X.; Li, J.; Hashmi, M.
786 L. U. R.; Liang, Y.; Li, T., Successive phytoextraction alters ammonia oxidation and
787 associated microbial communities in heavy metal contaminated agricultural soils. *Science of*
788 *the Total Environment* **2019,** *664*, 616-625.
789 28. Lu, L.; Tian, S.; Zhang, J.; Yang, X.; Labavitch, J. M.; Webb, S. M.; Latimer, M.; Brown,
790 P. H., Efficient xylem transport and phloem remobilization of Zn in the hyperaccumulator
791 plant species *Sedum alfredii*. *New Phytologist* **2013,** *198*, (3), 721-731.
792 29. Kafle, A.; Timilsina, A.; Gautam, A.; Adhikari, K.; Bhattarai, A.; Aryal, N.,
793 Phytoremediation: mechanisms, plant selection and enhancement by natural and synthetic
794 agents. *Environmental Advances* **2022,** *8*, 100203.

30. Veerapagu, M.; Jeya, K. R.; Sankaranarayanan, A., Role of plant growth-promoting microorganisms in phytoremediation efficiency. In *Plant-microbe interaction - recent advances in molecular and biochemical approaches*, Swapnil, P.; Meena, M.; Harish; Marwal, A.; Vijayalakshmi, S.; Zehra, A., Eds. Academic Press: 2023; pp 45-61.
31. Weiss, M.; Waller, F.; Zuccaro, A.; Selosse, M. A., Sebacinales - one thousand and one interactions with land plants. *New Phytologist* **2016,** *211*, (1), 20-40.
32. Zuccaro, A.; Lahrmann, U.; Guldener, U.; Langen, G.; Pfiffi, S.; Biedenkopf, D.; Wong, P.; Samans, B.; Grimm, C.; Basiewicz, M.; Murat, C.; Martin, F.; Kogel, K. H., Endophytic life strategies decoded by genome and transcriptome analyses of the mutualistic root symbiont *Piriformospora indica*. *PLoS Pathogens* **2011,** *7*, (10), e1002290.
33. Qiang, X.; Weiss, M.; Kogel, K. H.; Schaefer, P., *Piriformospora indica*-a mutualistic basidiomycete with an exceptionally large plant host range. *Molecular Plant Pathology* **2012,** *13*, (5), 508-518.
34. Varma, A.; Bakshi, M.; Lou, B.; Hartmann, A.; Oelmueller, R., *Piriformospora indica*: a novel plant growth-promoting mycorrhizal fungus. *Agricultural Research* **2012,** *1*, (2), 117-131.
35. Zuccaro, A.; Basiewicz, M.; Zurawska, M.; Biedenkopf, D.; Kogel, K. H., Karyotype analysis, genome organization, and stable genetic transformation of the root colonizing fungus *Piriformospora indica*. *Fungal Genetics and Biology* **2009,** *46*, (8), 543-550.
36. Shahabivand, S.; Parvaneh, A.; Aliloo, A. A., Root endophytic fungus *Piriformospora indica* affected growth, cadmium partitioning and chlorophyll fluorescence of sunflower under cadmium toxicity. *Ecotoxicology and Environmental Safety* **2017,** *145*, 496-502.
37. Rahman, S. u.; Khalid, M.; Hui, N.; Rehman, A.; Kayani, S.-I.; Fu, X.; Zheng, H.; Shao, J.; Khan, A. A.; Ali, M.; Taheri, A.; Liu, H.; Yan, X.; Hu, X.; Qin, W.; Peng, B.; Li, M.; Yao, X.; Zhang, Y.; Tang, K., *Piriformospora indica* alter root-associated microbiome structure to enhance *Artemisia annua* L. tolerance to arsenic. *Journal of Hazardous Materials* **2023,** *457*, 131752.
38. Li, D.; Zheng, X.; Lin, L.; An, Q.; Jiao, Y.; Li, Q.; Li, Z.; Hong, Y.; Zhang, K.; Xie, C.; Yin, J.; Zhang, H.; Wang, B.; Hu, Y.; Zhu, Z., Remediation of soils co-contaminated with cadmium and dichlorodiphenyltrichloroethanes by king grass associated with *Piriformospora indica*: insights into the regulation of root excretion and reshaping of rhizosphere microbial community structure. *Journal of Hazardous Materials* **2021,** *422*, 126936.
39. Zhang, K.; Zhang, H.; Xie, C.; Zhu, Z.; Lin, L.; An, Q.; Zhang, X.; Wu, W.; Li, D., *Piriformospora indica* colonization enhances remediation of cadmium and chromium co-contaminated soils by king grass through plant growth promotion and rhizosphere microecological regulation. *Journal of Hazardous Materials* **2023,** *462*, 132728.
40. Narayan, O. P.; Verma, N.; Jogawat, A.; Dua, M.; Johri, A. K., Sulfur transfer from the endophytic fungus *Serendipita indica* improves maize growth and requires the sulfate transporter *SiSulT*. *Plant Cell* **2021,** *33*, (4), 1268-1285.
41. Saleem, S.; Sekara, A.; Pokluda, R., *Serendipita indica*-A review from agricultural point of view. *Plants-Basel* **2022,** *11*, (24).
42. Hill, T. W.; Kafer, E., Improved protocols for *Aspergillus* minimal medium: trace element and minimal medium salt stock solutions. *Fungal Genetics Reports* **2001,** *48*, (1), 20-21.
43. Jiang, W.; Pan, R.; Wu, C.; Xu, L.; Abdelaziz, M. E.; Oelmuller, R.; Zhang, W.,

Piriformospora indica enhances freezing tolerance and post-thaw recovery in *Arabidopsis* by stimulating the expression of CBF genes. *Plant Signal Behav* **2020,** *15*, (4), 1745472.
44. Almario, J.; Jeena, G.; Wunder, J.; Langen, G.; Zuccaro, A.; Coupland, G.; Bucher, M., Root-associated fungal microbiota of nonmycorrhizal *Arabis alpina* and its contribution to plant phosphorus nutrition. *Proceedings of the National Academy of Sciences of the United States of America* **2017,** *114*, (44), E9403-E9412.
45. Tian, S.; Lu, L.; Yang, X.; Webb, S. M.; Du, Y.; Brown, P. H., Spatial imaging and speciation of lead in the accumulator plant *Sedum alfredii* by microscopically focused synchrotron X-ray investigation. *Environmental Science & Technology* **2010,** *44*, (15), 5920-6.
46. Cai, Z.; Lai, B.; Xiao, Y.; Xu, S., An X-ray diffraction microscope at the Advanced Photon Source. *Journal de Physique IV (Proceedings)* **2003,** *104*, 17-20.
47. Xie, R.; Zhao, J.; Lu, L.; Jernstedt, J.; Guo, J.; Brown, P. H.; Tian, S., Spatial imaging reveals the pathways of Zn transport and accumulation during reproductive growth stage in almond plants. *Plant Cell And Environment* **2021,** *44*, (6), 1858-1868.
48. Vogt, S., MAPS : a set of software tools for analysis and visualization of 3D X-ray fluorescence data sets. *Journal de Physique IV (Proceedings)* **2003,** *104*, 635-638.
49. Salas-González, I.; Reyt, G.; Flis, P.; Custódio, V.; Gopaulchan, D.; Bakhoum, N.; Dew, T. P.; Suresh, K.; Franke, R. B.; Dangl, J. L.; Salt, D. E.; Castrillo, G., Coordination between microbiota and root endodermis supports plant mineral nutrient homeostasis. *Science* **2021,** *371*, (6525).
50. Caporaso, J. G.; Lauber, C. L.; Walters, W. A.; Berg-Lyons, D.; Lozupone, C. A.; Turnbaugh, P. J.; Fierer, N.; Knight, R., Global patterns of 16S rRNA diversity at a depth of millions of sequences per sample. *Proceedings of the National Academy of Sciences of the United States of America* **2010,** *108*, (supplement_1), 4516-4522.
51. Bokulich, N. A.; Mills, D. A., Improved selection of internal transcribed spacer-specific primers enables quantitative, ultra-high-throughput profiling of fungal communities. *Applied and Environmental Microbiology* **2013,** *79*, (8), 2519-2526.
52. Dai, T.; Wen, D.; Bates, C. T.; Wu, L.; Guo, X.; Liu, S.; Su, Y.; Lei, J.; Zhou, J.; Yang, Y., Nutrient supply controls the linkage between species abundance and ecological interactions in marine bacterial communities. *Nature Communications* **2022,** *13*, (1), 175.
53. Bolyen, E.; Rideout, J. R.; Dillon, M. R.; Bokulich, N. A.; Abnet, C. C.; Al-Ghalith, G. A.; Alexander, H.; Alm, E. J.; Arumugam, M.; Asnicar, F.; Bai, Y.; Bisanz, J. E.; Bittinger, K.; Brejnrod, A.; Brislawn, C. J.; Brown, C. T.; Callahan, B. J.; Caraballo-Rodríguez, A. M.; Chase, J.; Cope, E. K.; Da Silva, R.; Diener, C.; Dorrestein, P. C.; Douglas, G. M.; Durall, D. M.; Duvallet, C.; Edwardson, C. F.; Ernst, M.; Estaki, M.; Fouquier, J.; Gauglitz, J. M.; Gibbons, S. M.; Gibson, D. L.; Gonzalez, A.; Gorlick, K.; Guo, J.; Hillmann, B.; Holmes, S.; Holste, H.; Huttenhower, C.; Huttley, G. A.; Janssen, S.; Jarmusch, A. K.; Jiang, L.; Kaehler, B. D.; Kang, K. B.; Keefe, C. R.; Keim, P.; Kelley, S. T.; Knights, D.; Koester, I.; Kosciolek, T.; Kreps, J.; Langille, M. G. I.; Lee, J.; Ley, R.; Liu, Y.; Loftfield, E.; Lozupone, C.; Maher, M.; Marotz, C.; Martin, B. D.; McDonald, D.; McIver, L. J.; Melnik, A. V.; Metcalf, J. L.; Morgan, S. C.; Morton, J. T.; Naimey, A. T.; Navas-Molina, J. A.; Nothias, L. F.; Orchanian, S. B.; Pearson, T.; Peoples, S. L.; Petras, D.; Preuss, M. L.; Pruesse, E.; Rasmussen, L. B.; Rivers, A.; Robeson, M. S.; Rosenthal, P.; Segata, N.; Shaffer, M.; Shiffer, A.; Sinha, R.; Song,

S. J.; Spear, J. R.; Swafford, A. D.; Thompson, L. R.; Torres, P. J.; Trinh, P.; Tripathi, A.; Turnbaugh, P. J.; Ul-Hasan, S.; van der Hooft, J. J. J.; Vargas, F.; Vázquez-Baeza, Y.; Vogtmann, E.; von Hippel, M.; Walters, W.; Wan, Y.; Wang, M.; Warren, J.; Weber, K. C.; Williamson, C. H. D.; Willis, A. D.; Xu, Z.; Zaneveld, J. R.; Zhang, Y.; Zhu, Q.; Knight, R.; Caporaso, J. G., Reproducible, interactive, scalable and extensible microbiome data science using QIIME 2. *Nature Biotechnology* **2019,** *37*, (8), 852-857.

54. Callahan, B. J.; McMurdie, P. J.; Rosen, M. J.; Han, A. W.; Johnson, A. J. A.; Holmes, S. P., DADA2: high-resolution sample inference from Illumina amplicon data. *Nature Methods* **2016,** *13*, (7), 581-3.

55. Quast, C.; Pruesse, E.; Yilmaz, P.; Gerken, J.; Schweer, T.; Yarza, P.; Peplies, J.; Glöckner, F. O., The SILVA ribosomal RNA gene database project: improved data processing and web-based tools. *Nucleic Acids Research* **2012,** *41*, (D1), D590-D596.

56. Kõljalg, U.; Larsson, K. H.; Abarenkov, K.; Nilsson, R. H.; Alexander, I. J.; Eberhardt, U.; Erland, S.; Høiland, K.; Kjøller, R.; Larsson, E.; Pennanen, T.; Sen, R.; Taylor, A. F. S.; Tedersoo, L.; Vrålstad, T.; Björn, M. U., UNITE: a database providing web-based methods for the molecular identification of ectomycorrhizal fungi. *New Phytologist* **2005,** *166*, (3), 1063-1068.

57. Xu, J.; Zheng, L.; Xu, L.; Wang, X., Uptake and allocation of selected metals by dominant vegetation in Poyang Lake wetland: from rhizosphere to plant tissues. *Catena* **2020,** *189*.

58. Wang, Y.; Xu, Y.; Liang, X.; Wang, L.; Sun, Y.; Huang, Q.; Qin, X.; Zhao, L., Soil application of manganese sulfate could reduce wheat Cd accumulation in Cd contaminated soil by the modulation of the key tissues and ionomic of wheat. *Science of the Total Environment* **2021,** *770*, 145328.

59. Lima-Mendez, G.; Faust, K.; Henry, N.; Decelle, J.; Colin, S.; Carcillo, F.; Chaffron, S.; Ignacio-Espinosa, J. C.; Roux, S.; Vincent, F.; Bittner, L.; Darzi, Y.; Wang, J.; Audic, S.; Berline, L.; Bontempi, G.; Cabello, A. M.; Coppola, L.; Cornejo-Castillo, F. M.; d'Ovidio, F.; De Meester, L.; Ferrera, I.; Garet-Delmas, M. J.; Guidi, L.; Lara, E.; Pesant, S.; Royo-Llonch, M.; Salazar, G.; Sanchez, P.; Sebastian, M.; Souffreau, C.; Dimier, C.; Picheral, M.; Searson, S.; Kandels-Lewis, S.; Gorsky, G.; Not, F.; Ogata, H.; Speich, S.; Stemmann, L.; Weissenbach, J.; Wincker, P.; Acinas, S. G.; Sunagawa, S.; Bork, P.; Sullivan, M. B.; Karsenti, E.; Bowler, C.; de Vargas, C.; Raes, J., Determinants of community structure in the global plankton interactome. *Science* **2015,** *348*, (6237), 1262073.

60. Noble, W. S., How does multiple testing correction work? *Nature Biotechnology* **2009,** *27*, (12), 1135-7.

61. Luo, F.; Zhong, J.; Yang, Y.; Scheuermann, R. H.; Zhou, J., Application of random matrix theory to biological networks. *Physics Letters A* **2006,** *357*, (6), 420-423.

62. Deng, Y.; Jiang, Y.; Yang, Y.; He, Z.; Luo, F.; Zhou, J., Molecular ecological network analyses. *BMC Bioinformatics* **2012,** *13*, 113.

63. Kundu, A.; Mishra, S.; Kundu, P.; Jogawat, A.; Vadassery, J., *Piriformospora indica* recruits host-derived putrescine for growth promotion in plants. *Plant Physiology* **2022**.

64. Cao, J.; He, W.; Zou, Y.; Wu, Q., An endophytic fungus, *Piriformospora indica*, enhances drought tolerance of trifoliate orange by modulating the antioxidant defense system and composition of fatty acids. *Tree Physiology* **2023,** *43*, (3), 452-466.

65. Sirrenberg, A.; Goebel, C.; Grond, S.; Czempinski, N.; Ratzinger, A.; Karlovsky, P.; Santos, P.; Feussner, I.; Pawlowski, K., *Piriformospora indica* affects plant growth by auxin production. *Physiologia Plantarum* **2007,** *131*, (4), 581-589.
66. Waller, F.; Achatz, B.; Baltruschat, H.; Fodor, J.; Becker, K.; Fischer, M.; Heier, T.; Huckelhoven, R.; Neumann, C.; von Wettstein, D.; Franken, P.; Kogel, K. H., The endophytic fungus *Piriformospora indica* reprograms barley to salt-stress tolerance, disease resistance, and higher yield. *Proceedings of the National Academy of Sciences of the United States of America* **2005,** *102*, (38), 13386-91.
67. Gill, S. S.; Gill, R.; Trivedi, D. K.; Anjum, N. A.; Sharma, K. K.; Ansari, M. W.; Ansari, A. A.; Johri, A. K.; Prasad, R.; Pereira, E.; Varma, A.; Tuteja, N., *Piriformospora indica*: potential and significance in plant stress tolerance. *Frontiers in Microbiology* **2016,** *7*, 332.
68. Kundu, A.; Vadassery, J., Molecular mechanisms of *Piriformospora indica* mediated growth promotion in plants. *Plant Signaling & Behavior* **2022,** *17*, (1), 2096785.
69. Hosseini, F.; Mosaddeghi, M. R.; Dexter, A. R.; Sepehri, M., Effect of endophytic fungus *Piriformospora indica* and PEG-induced water stress on maximum root growth pressure and elongation rate of maize. *Plant and Soil* **2018,** *435*, (1-2), 423-436.
70. Saleem, S.; Sekara, A.; Pokluda, R., *Serendipita indica*—a review from agricultural point of view. *Plants* **2022,** *11*, (24), 3417.
71. Pedersen, B. P.; Kumar, H.; Waight, A. B.; Risenmay, A. J.; Roe-Zurz, Z.; Chau, B. H.; Schlessinger, A.; Bonomi, M.; Harries, W.; Sali, A.; Johri, A. K.; Stroud, R. M., Crystal structure of a eukaryotic phosphate transporter. *Nature* **2013,** *496*, (7446), 533-536.
72. Sun, S.; Chen, J.; Zhao, F., Regulatory mechanisms of sulfur metabolism affecting tolerance and accumulation of toxic trace metals and metalloids in plants. *Journal of Experimental Botany* **2023,** *74*, (11), 3286-3299.
73. Gill, S. S.; Tuteja, N., Cadmium stress tolerance in crop plants: probing the role of sulfur. *Plant Signaling & Behavior* **2011,** *6*, (2), 215-22.
74. Yamaguchi, C.; Takimoto, Y.; Ohkama-Ohtsu, N.; Hokura, A.; Shinano, T.; Nakamura, T.; Suyama, A.; Maruyama-Nakashita, A., Effects of Cadmium Treatment on the Uptake and Translocation of Sulfate in *Arabidopsis thaliana*. *Plant And Cell Physiology* **2016,** *57*, (11), 2353-2366.
75. Baig, M. A.; Ahmad, J.; Ali, A. A.; Amna; Qureshi, M. I., Chapter 13 - Role of Sulfur Metabolism in Cadmium Tolerance. In *Cadmium Tolerance in Plants*, Hasanuzzaman, M.; Vara Prasad, M. N.; Nahar, K., Eds. Academic Press: 2019; pp 335-365.
76. Ashley, M. K.; Grant, M.; Grabov, A., Plant responses to potassium deficiencies: a role for potassium transport proteins. *Journal of Experimental Botany* **2006,** *57*, (2), 425-36.
77. Conchillo, L. B.; Haro, R.; Benito, B., K^+ Nutrition Exchange in the *Serendipita-Arabidopsis* Symbiosis: Study of the Fungal K^+ Transporters Involved. *Frontiers in Ecology and Evolution* **2021,** *9*.
78. Liu, C.; Lin, H.; Dong, Y.; Li, B., Increase of P and Cd bioavailability in the rhizosphere by endophytes promoted phytoremediation efficiency of *Phytolacca acinosa*. *Journal of Hazardous Materials* **2022,** *431*, 128546.
79. Zhang, S.; Sun, G.; Yin, X.; Rensing, C.; Zhu, Y., Biomethylation and volatilization of arsenic by the marine microalgae *Ostreococcus tauri*. *Chemosphere* **2013,** *93*, (1), 47-53.
80. Mohd, S.; Shukla, J.; Kushwaha, A. S.; Mandrah, K.; Shankar, J.; Arjaria, N.; Saxena, P.

971 N.; Narayan, R.; Roy, S. K.; Kumar, M., Endophytic fungi *Piriformospora indica* mediated
972 protection of host from arsenic toxicity. *Frontiers in Microbiology* **2017,** *8*, 754.
973 81. Zhao, F.; Jiang, R.; Dunham, S. J.; McGrath, S. P., Cadmium uptake, translocation and
974 tolerance in the hyperaccumulator *Arabidopsis halleri*. *New Phytologist* **2006,** *172*, (4),
975 646-54.
976 82. Shen, Z.; Zhao, F.; McGrath, S. P., Uptake and transport of zinc in the hyperaccumulator
977 *Thlaspi caerulescens* and the non-hyperaccumulator *Thlaspi ochroleucum*. *Plant, Cell and*
978 *Environment* **1997,** *20*, (7), 898-906.
979 83. Lasat, M. M.; Baker, A. J. M.; Kochian, L. V., Physiological characterization of root Zn^{2+}
980 absorption and translocation to shoots in Zn hyperaccumulator and nonaccumulator species of
981 Thlaspi. *Plant Physiology* **1996,** *112*, (4), 1715-1722.
982 84. Zhu, Z.; Yang, X.; Wang, K.; Huang, H.; Zhang, X.; Fang, H.; Li, T.; Alva, A. K.; He, Z.,
983 Bioremediation of Cd-DDT co-contaminated soil using the Cd-hyperaccumulator *Sedum*
984 *alfredii* and DDT-degrading microbes. *Journal of Hazardous Materials* **2012,** *235-236*,
985 144-51.
986 85. Ray, P.; Guo, Y.; Chi, M.-H.; Krom, N.; Boschiero, C.; Watson, B.; Huhman, D.; Zhao, P.;
987 Singan, V. R.; Lindquist, E. A.; Yan, J.; Adam, C.; Craven, K. D., *Serendipita fungi* modulate
988 the switchgrass root transcriptome to circumvent host defenses and establish a symbiotic
989 relationship. *Molecular Plant-Microbe Interactions* **2021,** *34*, (10), 1128-1142.
990 86. Wu, C.; Wei, Q.; Deng, J.; Zhang, W., Changes in gas exchange, root growth, and
991 biomass accumulation of *Platycladus orientalis* seedlings colonized by *Serendipita indica*.
992 *Journal of Forestry Research* **2018,** *30*, (4), 1199-1207.
993 87. Loha, A.; Kashyap, A. K.; Sharma, P., A putative cyclin, *SiPHO80* from root endophytic
994 fungus *Serendipita indica* regulates phosphate homeostasis, salinity and heavy metal toxicity
995 tolerance. *Biochemical and Biophysical Research Communications* **2018,** *507*, (1-4), 414-419.
996 88. Varma, A.; Kost, G.; Oelmüller, R., *Piriformospora indica*. Springer Berlin, Heidelberg:
997 **2013**.
998 89. Chen, T.; Liu, X.; Zhang, X.; Chen, X.; Tao, K.; Hu, X., Effect of alkyl polyglucoside
999 and nitrilotriacetic acid combined application on lead/pyrene bioavailability and
1000 dehydrogenase activity in co-contaminated soils. *Chemosphere* **2016,** *154*, 515-520.
1001 90. Jiang, W.; He, J.; Babla, M.; Wu, T.; Tong, T.; Riaz, A.; Zeng, F.; Qin, Y.; Chen, G.; Deng,
1002 F.; Chen, Z.H., Molecular evolution and interaction of 14-3-3 proteins with H^+-ATPases in
1003 plant abiotic stresses. *Journal of Experimental Botany* **2023**, erad414.
1004 91. Whiting, S. N.; de Souza, M. P.; Terry, N., Rhizosphere bacteria mobilize Zn for
1005 hyperaccumulation by *Thlaspi caerulescens*. *Environmental Science & Technology* **2001,** *35*,
1006 (15), 3144-50.
1007 92. Fomina, M. A.; Alexander, I. J.; Colpaert, J. V.; Gadd, G. M., Solubilization of toxic
1008 metal minerals and metal tolerance of mycorrhizal fungi. *Soil Biology and Biochemistry* **2005,**
1009 *37*, (5), 851-866.
1010 93. Li, X.; Yu, H.; Sun, X.; Yang, J.; Wang, D.; Shen, L.; Pan, Y.; Wu, Y.; Wang, Q.; Zhao, Y.,
1011 Effects of sulfur application on cadmium bioaccumulation in tobacco and its possible
1012 mechanisms of rhizospheric microorganisms. *Journal of Hazardous Materials* **2019,** *368*,
1013 308-315.
1014 94. Wang, S.; Niu, X.; Di, D.; Huang, D., Nitrogen and sulfur fertilizers promote the

absorption of lead and cadmium with *Salix integra* Thunb. by increasing the bioavailability of heavy metals and regulating rhizosphere microbes. *Frontiers in Microbiology* **2022,** *13*.
95. Netherway, T.; Bengtsson, J.; Buegger, F.; Fritscher, J.; Oja, J.; Pritsch, K.; Hildebrand, F.; Krab, E. J.; Bahram, M., Pervasive associations between dark septate endophytic fungi with tree root and soil microbiomes across Europe. *Nature Communications* **2024,** *15*, (1), 159.
96. Meyer, B.; Imhoff, J. F.; Kuever, J., Molecular analysis of the distribution and phylogeny of the *soxB* gene among sulfur-oxidizing bacteria - evolution of the Sox sulfur oxidation enzyme system. *Environmental Microbiology* **2007,** *9*, (12), 2957-77.
97. Li, X.; Sato, T.; Ooiwa, Y.; Kusumi, A.; Gu, J.; Katayama, Y., Oxidation of elemental sulfur by *Fusarium solani* strain THIF01 harboring endobacterium *Bradyrhizobium* sp. *Microbial Ecology* **2010,** *60*, (1), 96-104.
98. Kumar, R.; Verma, H.; Haider, S.; Bajaj, A.; Sood, U.; Ponnusamy, K.; Nagar, S.; Shakarad, M. N.; Negi, R. K.; Singh, Y.; Khurana, J. P.; Gilbert, J. A.; Lal, R., Comparative genomic analysis reveals habitat-specific genes and regulatory hubs within the genus *Novosphingobium*. *mSystems* **2017,** *2*, (3), e00020-17.
99. Santana, M. M.; Dias, T.; Gonzalez, J. M.; Cruz, C., Transformation of organic and inorganic sulfur–adding perspectives to new players in soil and rhizosphere. *Soil Biology and Biochemistry* **2021,** *160*, 108306.
100. Schmalenberger, A.; Hodge, S.; Bryant, A.; Hawkesford, M. J.; Singh, B. K.; Kertesz, M. A., The role of *Variovorax* and other *Comamonadaceae* in sulfur transformations by microbial wheat rhizosphere communities exposed to different sulfur fertilization regimes. *Environmental Microbiology* **2008,** *10*, (6), 1486-500.
101. Ni, C.; Horton, D. J.; Rui, J.; Henson, M. W.; Jiang, Y.; Huang, X.; Learman, D. R., High concentrations of bioavailable heavy metals impact freshwater sediment microbial communities. *Annals of Microbiology* **2015,** *66*, (3), 1003-1012.
102. Yuan, Q.; Wang, P.; Wang, X.; Hu, B.; Tao, L., Phytoremediation of cadmium-contaminated sediment using *Hydrilla verticillata* and *Elodea canadensis* harbor two same keystone rhizobacteria *Pedosphaeraceae* and *Parasegetibacter*. *Chemosphere* **2022,** *286*, (Pt 1), 131648.
103. Chaintreuil, C.; Giraud, E.; Prin, Y.; Lorquin, J.; Ba, A. M.; Gillis, M.; de Lajudie, P.; Dreyfus, B., Photosynthetic bradyrhizobia are natural endophytes of the African wild rice *Oryza breviligulata*. *Applied and Environmental Microbiology* **2000,** *66*, (12), 5437-47.
104. Hayat, R.; Ali, S.; Amara, U.; Khalid, R.; Ahmed, I., Soil beneficial bacteria and their role in plant growth promotion: a review. *Annals of Microbiology* **2010,** *60*, (4), 579-598.
105. Deng, Y.; Fu, S.; Sarkodie, E. K.; Zhang, S.; Jiang, L.; Liang, Y.; Yin, H.; Bai, L.; Liu, X.; Liu, H.; Jiang, H., Ecological responses of bacterial assembly and functions to steep Cd gradient in a typical Cd-contaminated farmland ecosystem. *Ecotoxicology and Environmental Safety* **2022,** *229*, 113067.
106. Luo, J.; Gu, S.; Guo, X.; Liu, Y.; Tao, Q.; Zhao, H.; Liang, Y.; Banerjee, S.; Li, T., Core microbiota in the rhizosphere of heavy metal accumulators and its contribution to plant performance. *Environmental Science & Technology* **2022,** *56*, (18), 12975-12987.
107. Trivedi, P.; Leach, J. E.; Tringe, S. G.; Sa, T.; Singh, B. K., Plant-microbiome interactions: from community assembly to plant health. *Nature Reviews Microbiology* **2020,**

18, (11), 607-621.
108. Toju, H.; Peay, K. G.; Yamamichi, M.; Narisawa, K.; Hiruma, K.; Naito, K.; Fukuda, S.; Ushio, M.; Nakaoka, S.; Onoda, Y.; Yoshida, K.; Schlaeppi, K.; Bai, Y.; Sugiura, R.; Ichihashi, Y.; Minamisawa, K.; Kiers, E. T., Core microbiomes for sustainable agroecosystems. *Nature Plants* **2018,** *4*, (5), 247-257.
109. Newman, M. E. J., Fast algorithm for detecting community structure in networks. *Physical Review E - Statistical, Nonlinear, and Soft Matter Physics* **2004,** *69*, (6 Pt 2), 066133.
110. Newman, M. E. J., Modularity and community structure in networks. *Proceedings of the National Academy of Sciences of the United States of America* **2006,** *103*, (23), 8577-82.
111. Qiu, L.; Zhang, Q.; Zhu, H.; Reich, P. B.; Banerjee, S.; van der Heijden, M. G. A.; Sadowsky, M. J.; Ishii, S.; Jia, X.; Shao, M.; Liu, B.; Jiao, H.; Li, H.; Wei, X., Erosion reduces soil microbial diversity, network complexity and multifunctionality. *ISME Journal* **2021,** *15*, (8), 2474-2489.
112. Fesel, P. H.; Zuccaro, A., Dissecting endophytic lifestyle along the parasitism/mutualism continuum in *Arabidopsis*. *Current Opinion in Microbiology* **2016,** *32*, 103-112.
113. Fields, B.; Friman, V. P., Microbial eco-evolutionary dynamics in the plant rhizosphere. *Current Opinion in Microbiology* **2022,** *68*, 102153.
114. Agler, M. T.; Ruhe, J.; Kroll, S.; Morhenn, C.; Kim, S. T.; Weigel, D.; Kemen, E. M., Microbial hub taxa link host and abiotic factors to plant microbiome variation. *PLOS Biology* **2016,** *14*, (1), e1002352.
115. de Vries, F. T.; Griffiths, R. I.; Bailey, M.; Craig, H.; Girlanda, M.; Gweon, H. S.; Hallin, S.; Kaisermann, A.; Keith, A. M.; Kretzschmar, M.; Lemanceau, P.; Lumini, E.; Mason, K. E.; Oliver, A.; Ostle, N.; Prosser, J. I.; Thion, C.; Thomson, B.; Bardgett, R. D., Soil bacterial networks are less stable under drought than fungal networks. *Nature Communications* **2018,** *9*, (1), 3033.
116. Chen, Y.; Ding, Q.; Chao, Y.; Wei, X.; Wang, S.; Qiu, R., Structural development and assembly patterns of the root-associated microbiomes during phytoremediation. *Science of the Total Environment* **2018,** *644*, 1591-1601.
117. Wen, T.; Yuan, J.; He, X.; Lin, Y.; Huang, Q.; Shen, Q., Enrichment of beneficial cucumber rhizosphere microbes mediated by organic acid secretion. *Horticulture Research* **2020,** *7*, 154.
118.Belimov, A. A.; Hontzeas, N.; Safronova, V. I.; Demchinskaya, S. V.; Piluzza, G.; Bullitta, S.; Glick, B. R., Cadmium-tolerant plant growth-promoting bacteria associated with the roots of Indian mustard (*Brassica juncea* L. Czern.). *Soil Biology and Biochemistry* **2005,** *37*, (2), 241-250.
119. Bal, H. B.; Das, S.; Dangar, T. K.; Adhya, T. K., ACC deaminase and IAA producing growth promoting bacteria from the rhizosphere soil of tropical rice plants. *Journal of Basic Microbiology* **2013,** *53*, (12), 972-84.